Variation of seasonal wood growth in the Central-African semi-decidious forest of the Luki Biosphere Reserve.

Auteur : Dewez, Meven
Promoteur(s) : De Mil, Tom; Kaddouri, Marjane
Faculté : Gembloux Agro-Bio Tech (GxABT)
Diplôme : Master en bioingénieur : gestion des forêts et des espaces naturels, à finalité spécialisée
Année académique : 2024-2025
URI/URL : http://hdl.handle.net/2268.2/24057

LIÈGE université
Gembloux
Agro-Bio Tech

VARIATION OF SEASONAL WOOD GROWTH IN THE CENTRAL-AFRICAN SEMI-DECIDIOUS FOREST OF THE LUKI BIOSPHERE RESERVE (DRC)

MEVEN DEWEZ

TRAVAIL DE FIN D'ETUDES PRESENTE EN VUE DE L'OBTENTION DU DIPLOME DE MASTER BIOINGENIEUR EN GESTION DES FORETS ET ESPACES NATURELS

ANNEE ACADEMIQUE 2024-2025

CO-PROMOTEURS : PR. DE MIL TOM ET KADDOURI MARJANE

[1] The academic authority is represented by the thesis supervisor, a member of the GxABT teaching staff.

[2] L'autorité académique est représentée par les promoteurs membre du personnel enseignant de GxABT.

LIÈGE université
Gembloux
Agro-Bio Tech

VARIATION OF SEASONAL WOOD GROWTH IN THE CENTRAL-AFRICAN SEMI-DECIDIOUS FOREST OF THE LUKI BIOSPHERE RESERVE (DRC)

MEVEN DEWEZ

TRAVAIL DE FIN D'ETUDES PRESENTE EN VUE DE L'OBTENTION DU DIPLOME DE MASTER BIOINGENIEUR EN GESTION DES FORETS ET ESPACES NATURELS

ANNEE ACADEMIQUE 2024-2025

CO-PROMOTEURS : PR. DE MIL TOM ET KADDOURI MARJANE

Acknowledgements

I would first like to express my sincere gratitude to my supervisors, Kaddouri Marjane and Professor Tom De Mil, for their guidance and the time they invested to ensure the success of this study.

I am especially grateful to Dr Adeline Fayolle, who, even after leaving her teaching role at Gembloux, made herself available to offer support and advice.

My warm thanks also go to Professor Bhely Angoboy Ilondea for his welcome and the trust he placed in me during my internship in the Democratic Republic of Congo. I also wish to thank the field teams who supported me over the course of three months and made everything possible in the field. I am particularly grateful to Steve, Fils, Placide, Grace and Tsuke, without whom I would not have been able to explore the CANOPi research setup, which forms the foundation of this work.

I will be forever thankful for the support my mother has given me every day and throughout my life. Thank you for listening, for understanding, for providing for me, and for putting up with my mistakes despite the difficulties.

I would like to warmly thank the friends and "Abbaystes" who stood by me during what have been the two most beautiful years of my life so far, and who helped me stay the course with my studies. I am especially thankful to the 2021 team, Spiroux, Virgi, Babette, Grygry and Gipsy, who witnessed my first steps in this wonderful family, and to my own team, 2022, Babette, Gipsy, Marypleine, Buisson and Dernier. I will never forget you.

Within this AGéenne journey, I have also had the chance to meet friends with whom I led the 2022 AG project. Spiroux, Tinmar, Dina, Floche, Verjaune, bArBI, Charline and Tony, your support was invaluable and this year will remain engraved in my memory.

Finally, I want to thank my friends Alex, Thomas, Cameron, Eliott, Samuel, De Was, Matthias, Antoine, Tom, Bourlon, Ghislain and many others not mentioned here. Life would have been much duller without you.

Abstract

Understanding the seasonal dynamics of radial growth in tropical trees is essential for predicting forest responses to climate change. This study, conducted within the framework of the CANOPi project, investigated growth patterns in canopy trees from the Luki Biosphere Reserve (DRC) using high-resolution dendrometer data collected over 20 months. Growth curves were classified into distinct patterns through breakpoint analysis, and their relationships with tree traits (e.g. diameter, wood density, leaf habit) and climatic variables from ERA5 were explored. Four growth types were identified: highly seasonal, moderately seasonal, non-seasonal, and no-growth, with deciduous species largely dominating the seasonal groups. Strong inter- and intra-specific variability was observed in growth period timing, duration, and intensity. The growth period of seasonal patterns was closely aligned with the wet season, with growth onset and cessation largely driven by rainfall and soil water content thresholds. Non-seasonal trees were predominantly evergreen or exhibited potential rapid leaf exchange. Gompertz modelling of the highly seasonal group revealed a consistent inflection point between January and February, coinciding with a brief dry spell within the wet season. These findings confirm the strong climatic control over growth seasonality in Central African forests and highlight the need to integrate fine-scale monitoring with phenological and anatomical analyses to improve growth modelling under changing climate conditions.

Résumé

Comprendre la dynamique saisonnière de la croissance radiale des arbres tropicaux est essentiel pour prédire la réponse des forêts au changement climatique. Cette étude, menée dans le cadre du projet CANOPi, a analysé les schémas de croissance d'arbres de canopée de la Réserve de biosphère de Luki (RDC) à partir de données de dendromètres à haute résolution collectées sur 20 mois. Les courbes de croissance ont été classées en différents types grâce à une analyse « *breakpoints* », et leurs relations avec les caractéristiques des arbres (diamètre, densité du bois, phénologie foliaire) ainsi qu'avec les variables climatiques issues d'ERA5 ont été examinées. Quatre types de schémas de croissance ont été identifiés : fortement saisonnier (*highly seasonal*), modérément saisonnier (*moderately seasonal*), non saisonnier (*non-seasonal*) et absence de croissance (*no growth*), les espèces décidues dominant largement les groupes saisonniers. Une forte variabilité inter- et intra-spécifique a été observée dans la durée et l'intensité des périodes de croissance. Les périodes de croissances des schémas saisonniers coïncident étroitement avec la saison humide, avec un déclenchement et un arrêt de la croissance principalement déterminés par les précipitations et les seuils de teneur en eau du sol. Les arbres non saisonniers étaient principalement sempervirents ou présentaient potentiellement un comportement qualifié de « *leaf exchanger* ». La modélisation de Gompertz appliquée au groupe fortement saisonnier a révélé un point d'inflexion constant entre janvier et février, correspondant à une courte saison sèche à l'intérieur de la saison humide. Ces résultats montrent l'influence majeure du climat sur la saisonnalité de la croissance en Afrique centrale et soulignent l'importance de combiner un suivi détaillé avec des analyses phénologiques et anatomiques pour affiner la modélisation de la croissance face au changement climatique.

Table of contents

Acknowledgements I

Abstract II

Résumé III

List of Figures VI

List of appendix IX

List of Abbreviations XI

1. Introduction 1

1.1. Climate change and tropical forest functioning 1

1.2. Rainfall-driven seasonality in Central Africa 4

1.3. Tree stem growth as an indicator of environmental response 6

1.4. Research objectives 7

2. Material and methods 9

2.1. Study site 9

2.2. Data collection 10

2.3. Data cleaning 12

2.4. Growth patterns 16

2.5. Community-level trends 18

2.6. Breakpoint analysis 19

2.7. Inter- and intra-species variations 21

2.8. Link between growth and environmental conditions 22

2.9. Gompertz modelling 23

3. Results 25

3.1. Community-level trends 25

3.2. Wood growth patterns 27

3.3. Breakpoint analysis 31

3.4. Inter- and intra-specific variations 36
3.5. Link between growth and environmental conditions 37
3.6. Gompertz modelling 42
4. Discussion and perspectives 44
4.1. Community-level growth trends 44
4.2. Seasonal growth patterns: dynamics and variability 45
4.3. Climatic and environmental influence 48
4.4. Additional insights from Gompertz growth modelling 49
5. Conclusion 51
6. Personal contribution 52
7. References 53
8. Appendix 64

List of Figures

Figure 1.1: Importance of tropical forests for carbon stocks. Biome distributions and carbon stored by biome adapted from Rachel (2014)..... 2
Figure 1.2: Climate and topography of the Guineo-Congolian regional centre of endemism from White (1983). 4
Figure 1.3: (A) Map of the number of dry months per year in Africa, and (B) the UNESCO vegetation map of Africa (Bouvet et al., 2018)..... 5
Figure 2.1: (A)The study site: Luki Biosphere Reserve (UNESCO MAB located by a red dot. The background map is the land cover classification from the Digital Earth Africa platform. (B) Ombrothermic diagrams (data from NASA POWER platform) of the study site. 10
Figure 2.2: Scheme of a TOMST point dendrometer 11
Figure 2.3: Orthophoto acquired by drone, showing the locations of the different phenocams and the trees equipped with dendrometers in the Luki Biosphere Reserve. 12
Figure 2.4: (A) The three distinct phases of the stem radius variation: growth (green), shrinkage (red) and swelling (orange) (Luse et al. 2024). (B) Zoom on the growth period (between 10 and 19 April 2024) of a tree (92232071 – *Dialium pachyphyllum*) showing these three distinct phases represented with same legend as in panel A..... 13
Figure 2.5: Data cleaning framework on a tree (dendrometer 92232071 – *Dialium pachyphyllum*):(A) Big negative jumps due to recalibration cleaning framed in red and the same cumulative radial growth curve without the jump, (B) illustration of a minor discontinuity resulting from field data collection operations and (C) cleaned cumulative radial growth curve. 15
Figure 2.6: Decision tree of the visual approach developed to characterise growth patterns..... 17
Figure 2.7: Illustration of two individuals (A: dendrometer 92232003 – *Zanha golungensis* (HS); B: dendrometer 92232029 – *Piptadeniastrum africanum* (MS)) with their selected breakpoints. Red markers indicate acceleration breakpoints, while yellow markers indicate stagnation breakpoints. 20
Figure 3.1: Mean trend growth curve with associated standard deviation, illustrating the overall growth dynamics among the 26 trees retained in the study..... 25

Figure 3.2: Distributions of basal area (m²), wood density (g/cm³) and absolute growth (µm) in the studied community. Boxes show the median, interquartile range and extremes. Scales differ by variable. 26
Figure 3.3: Cumulative radial growth (µm) of monitored trees grouped into four growth patterns: highly seasonal (top left), moderately seasonal (topright), non-seasonal (bottom left), and no-growth (bottom right). Each line represents the smoothed growth curve of an individual tree, colour-coded by species. 28
Figure 3.4: Mean cumulative radial growth (left) and monthly increments (µm/14 days aggregated per month) (right) for the three identified growth patterns: A = highly seasonal, B = moderately seasonal, C = non-seasonal. Green lines show LOESS trends (span = 0.3) with standard deviation in shading; boxplots display monthly increment distributions. 30
Figure 3.5: Growth periods of trees with a Highly Seasonal pattern, sorted by total absolute growth. Each horizontal line represents the duration of the growth phase between the start and end day of year (DOY), with the number of growth days indicated above the line. Species names and dendrometer IDs are displayed at the end of each line. The DOY axis spans from August 2023 to August 2024, with 2024 DOYs adjusted by +365 for continuity. The Y-axis indicates the total absolute growth (µm) over the growth period. 32
Figure 3.6: Growth periods of trees with a moderately seasonal pattern, sorted by total absolute growth. Each horizontal line represents the duration of the growth phase between the start and end day of year (DOY), with the number of growth days indicated above the line. Species names and dendrometer IDs are displayed at the end of each line. The DOY axis spans from August 2023 to August 2024, with 2024 DOYs adjusted by +365 for continuity. The Y-axis indicates the total absolute growth (µm) over the growth period. 34
Figure 3.7: Boxplots showing the distribution of two tree traits: basal area (m²) (A), and wood density (B) (g/cm³) across the three growth pattern categories: Highly Seasonal (HS), Moderately Seasonal (MS), and Non-Seasonal (NS). Individual points represent tree-level measurements. The Kruskal-Wallis p-values, shown above each plot, indicate whether trait distributions significantly differ among the groups. 36
Figure 3.8: Boxplots show the distribution of absolute growth for each species, with individual measurements represented as points. This visualisation highlights both the variability among species and the range of growth responses within species 37

Figure 3.9: Multi-layered plot showing the relationship between the mean trend curve of the three patterns and various environmental variables. Precipitation (mm), relative humidity (RH, %), net surface radiation (W/m²), maximum VPD (hPa), temperature (°C) and volumetric soil water content (VSWC; m³/m³) at different depths (0–7 cm, 7–28 cm, 28–100 cm, and 100–255 cm). Environmental data were extracted from the ERA5 database. 39
Figure 3.10: Monthly correlations between average growth of the different patterns and key environmental variables. Each panel shows the Pearson correlation coefficient between monthly growth and a given environmental variable, calculated for each year of monitoring. Variables include net radiation (W/m²), total precipitation (mm), relative humidity (%), volumetric soil water content (VSWC) at different depths (0–7 cm, 7–28 cm, 28–100 cm, 100–255 cm), air temperature (°C), and vapour pressure deficit (VPD, hPa). Red dashed lines indicate the beginning of the main growth period and blue dashed lines indicate the end of the period. 41
Figure 3.11: Hierarchical Gompertz fit (green) with confidence bands (grey) for highly seasonal trees (biweekly data). Grey dots: individual dendrometer measurements (relative growth, %). Vertical dashed line: inflection point; shaded area: 5–95% growth period..... 42
Figure 4.1: Cross section of 6 trees within the 3 patterns: (A.1) *Zanha golugensis* and (A.2) *Prioria balsamifera* as highly seasonal, (B.1) *Piptadenisatrum africanum* and (B.2) *Miliciea excelsa* as moderately seasonal, (C.1) *Guarea cedrata* and (C.2) Ongokea gore. Picture come from InsideWood data base. 46

List of appendix

Figure A1: Increment curves recorded by a dendrometer (92232083 – *Desbordesia glaucescens*), which shows saturation highlighted in red and is therefore excluded from the study. 64
Figure A2: Examples of three dendrometer curves classified as 'others' and excluded from the analyses conducted in this study 65
Figure A3: Boxplots showing the distribution of absolute growth (µm) across different leaf habits (evergreen and deciduous) (a) and growth patterns (Highly seasonal - HS, Moderately seasonal - MS, and Non-seasonal - NS) (b). Kruskal-Wallis (a) and Wilcoxon rank-sum (b) tests were performed to assess group differences, with associated p-values reported..... 66
Table A1: Summary table of the trees selected after data cleaning, including the dendrometer ID, species, family, leaf habit (deciduous or evergreen), seasonal growth pattern (Highly seasonal - HS, Moderately seasonal - MS, or Non-seasonal - NS), diameter at breast height (DBH, cm), height (H, m), basal area (m²), wood density (g/cm³), and absolute growth over the full data period (in µm). The asterisks indicate that both dendrometers are installed on the same tre 67
Figure A4: Scatterplots illustrating the relationships between absolute growth (µm) and diameter at breast height (DBH, a), wood density (g/cm³, b), and height (m, c). Each point represents one tree. These plots aim to visualise variability and explore potential trends between the variables..... 68
Table A2: Mean, minimum and maximum score of the breakpoint detected and selected 69
Table A3: Key metrics from the breakpoint analysis for each tree exhibiting a highly seasonal pattern: the day of year marking the start (start DOY) and end (end DOY) of the growth period, the number of growth days (nGROW), the growth rate (GR, in µm/day), and the absolute growth (in µm) during the growth period from August 2023 to August 2024..... 70
Table A4: Key metrics from the breakpoint analysis for each tree exhibiting a moderately seasonal pattern: the day of year marking the start (start DOY) and end (end DOY) of the growth period, the number of growth days (nGROW), the growth rate (GR, in µm/day), and the absolute growth (in µm) during the growth period from August 2023 to August 2024..... 71

Table A5: Key metrics for each tree exhibiting a non-seasonal pattern: the growth rate (GR, in µm/day) and the absolute growth (in µm), calculated over the entire study period..... 71
Figure A5: Gompertz model for all the species classified highly seasonal: (A) *Albizia ferruginea*, (B) *Irvingia gobensis*, (C) *Prioria Balsamifera*, (D) *Pterocarpus tinctorius*, (E) *Terminalia superba*, (F) *Albizia gummifera*, (G) *Dialium pachyphyllum* and (H) *Zanha golugensis*. 72

List of Abbreviations

ITCZ: Intertropical Convergence Zone

DRC: Democratic Republic of Congo

CANOPi: Central African Network of Observatories of troPIcal

DBH: Diameter at breast height

DOY: Day Of Year

VPD: Vapour Pressure Deficit

RH: Relative Humidity

VSWC: Volumetric Soil Water Content

RMSE: Root Mean Square Error

ID: Identifier

GR: Grow rate

HS: Highly Seasonal

MS: Moderately Seasonal

NS: Non-Seasonal

AI: Artificial Intelligence

1. Introduction

1.1. Climate change and tropical forest functioning

Climate change is one of the most significant threats to global biodiversity and ecosystem functioning (Thomas et al., 2004; Román-Palacios & Wiens, 2020). The natural world is reshaped by rising temperatures, altered precipitation patterns, and an increased frequency of extreme weather events. These changes lead to widespread disturbances across ecosystems. Species have experienced shifts in their geographic distributions (Root et al., 2003; Uddin & Chaudhry, 2024) and in their phenological traits (Uddin & Chaudhry, 2024; Fayaz et al., 2025), and are also facing an increased risk of extinction (Thomas et al., 2004; Román-Palacios & Wiens, 2020).

As a cascade effect, ecosystems undergo changes in their dynamics due to climate change and the alterations of their species composition. Forest ecosystems are specifically threatened, despite the wide range of ecosystem services they provide. They contribute significantly to the global economy, offer habitats for wildlife, sustain natural cycles, and regulate the climate (Lindquist et al., 2012; Hui et al., 2017). It is important to note that forests represent the largest terrestrial carbon sink, and their integrity is crucial to mitigating the effects of climate change (Chen et al., 2021). This is why studying how forests respond to climate change is so important.

As tropical forests make up the majority of the world's forested area, they play a crucial role in regulating the global climate. They are key players in carbon cycling (figure 1.1) and significantly influence global climate patterns, representing 50% of terrestrial carbon stocks across 30% of the Earth's surface (Artaxo et al., 2022; Cusack et al., 2024). Tropical forests are also major global reservoirs of biodiversity, hosting between 50% and 80% of all terrestrial species (Lewis et al., 2009; Rachel, 2014; J. Wang et al., 2020). In addition, tropical forests are economically valuable, with an estimated worth of billions of US dollars (Yaduv et al., 2018). All these critical features highlight the need to study tropical forests in order to understand their resilience to climate change and ensure the continued delivery of the ecosystem services they provide (Cavaleri et al., 2015).

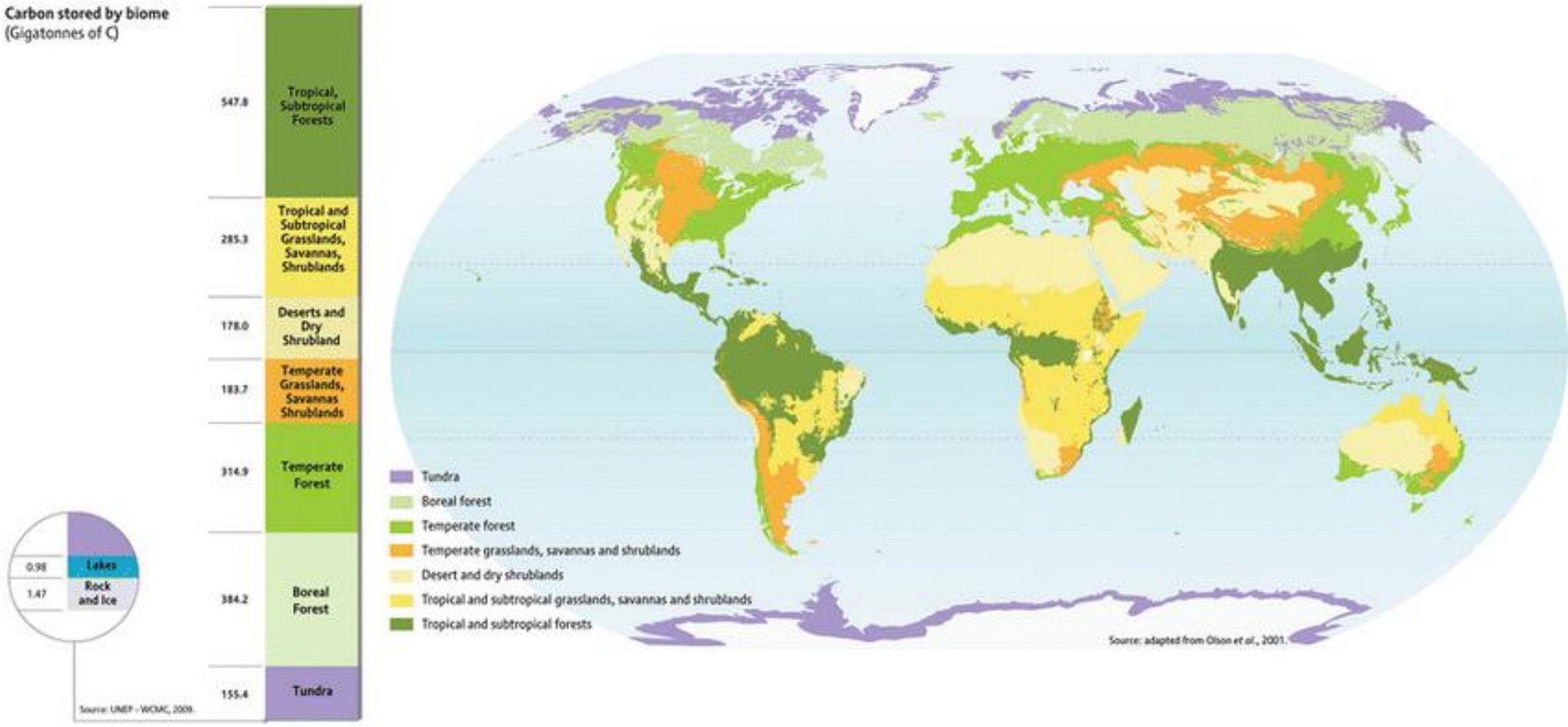

Figure 1.1: Importance of tropical forests for carbon stocks. Biome distributions and carbon stored by biome adapted from Rachel (2014)

The Congo Basin is the second largest continuous block of tropical forests in the world, after the Amazon Basin (Mayaux et al., 2013). The Congo Basin forest is among the most biologically rich ecosystems (Harrison et al., 2016), 4 times richer in woody plant species than the Amazon (Silva de Miranda et al., 2022). Taking this into account, along with the role of tropical forests in carbon storage (Rachel, 2014), and the share represented by the Congo Basin forest, this region therefore plays a major role in biodiversity conservation and global climate regulation (Hubau et al., 2020). The Congo Basin carbon sink capacity will decrease in a longer, lagged period compared to the Amazon Basin (Hubau et al., 2020). However, among the major tropical basins, the tropical moist forest of Central Africa has shown resilience to extreme climatic events such as El Niño (2015–2016) (Bennett et al., 2021). These Central African forests support several million people whose daily basic needs depend on them (L. J. T. White et al., 2021). Hence, it is vital to study the resilience of this forest (Cavaleri et al., 2015).

1.2. Rainfall-driven seasonality in Central Africa

In Central Africa, climate seasonality is mainly driven by the alternation between dry and wet seasons. This is primarily due to the convergence of the Intertropical Convergence Zone (ITCZ) around the equator, which is the main driver of precipitation in Central Africa (Tiersmondo Longandjo & Rouault, 2023).

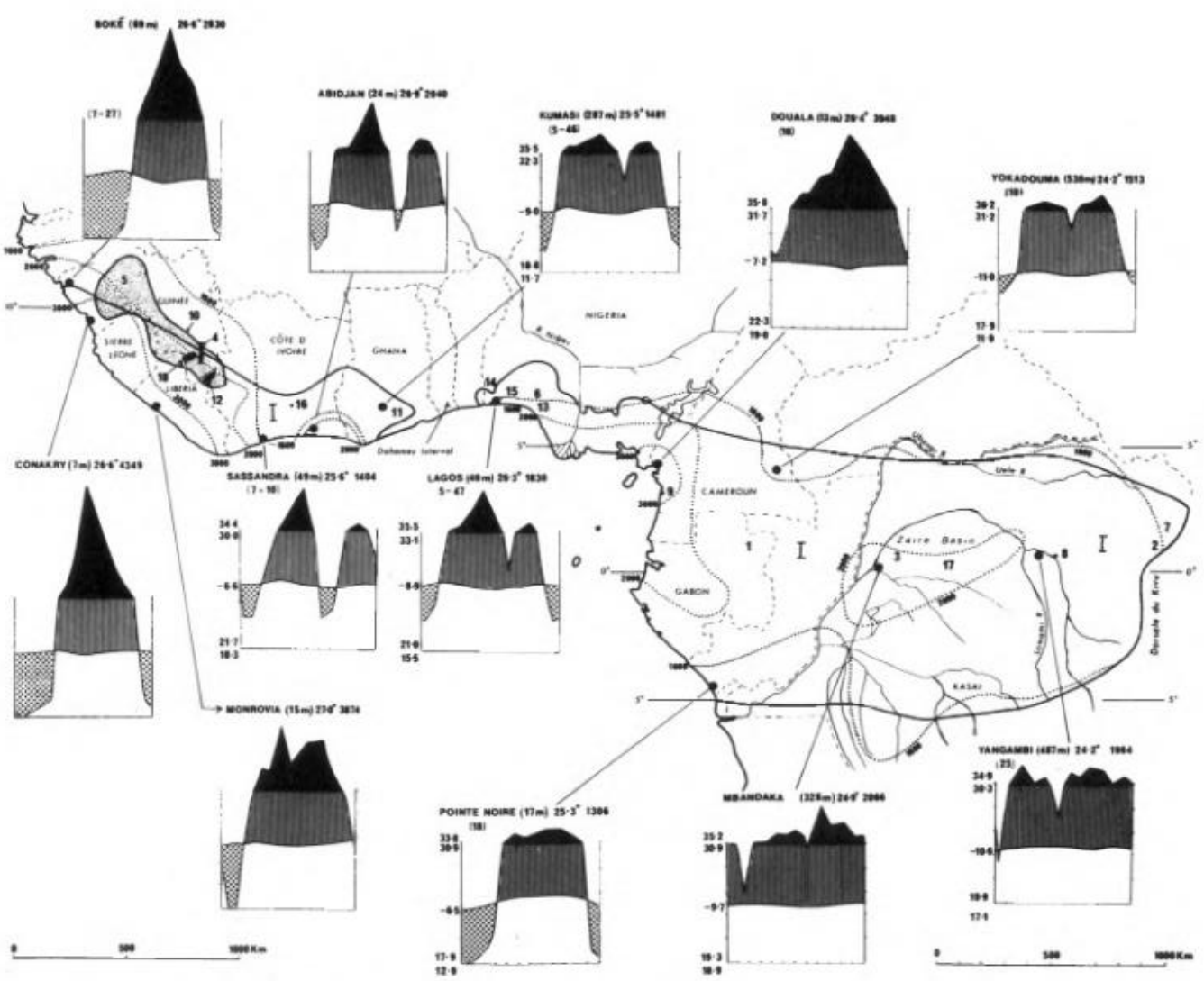

Figure 1.2: Climate and topography of the Guineo-Congolian regional centre of endemism from White (1983).

In contrast, temperature seasonality is minimal. Indeed, temperatures never drop below 18°C in lowland forests, as the region is predominantly classified as type A in the Köppen–Geiger climate classification (Peel et al., 2007; Beck et al., 2018).

Water availability is therefore a limiting factor in the composition of biomes in Central Africa (F. White, 1983). The figure below (figure 1.3) illustrates this variation in biomes according to the alternation between dry and wet seasons. It is clear that the dominant Central-African and most relevant biome here, tropical rainforest, is strongly associated with areas where the dry seasons are shortest (Bouvet et al., 2018).

A

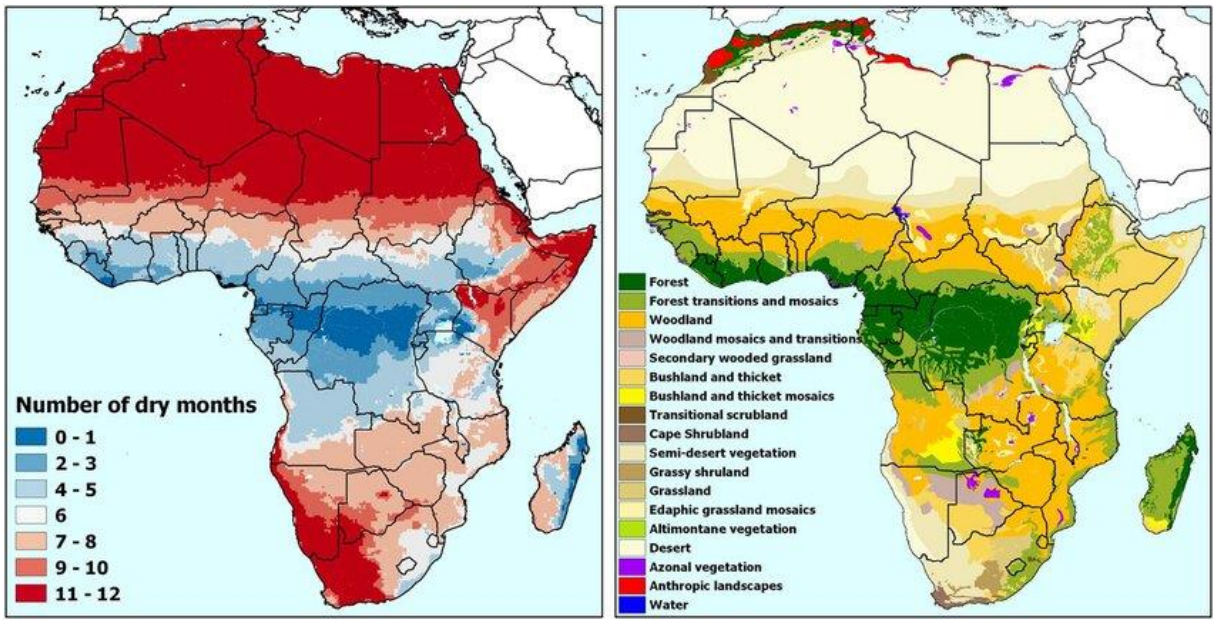

B

Figure 1.3: (A) Map of the number of dry months per year in Africa, and (B) the UNESCO vegetation map of Africa (Bouvet et al., 2018).

In Central Africa, that has drier and more seasonal climates than the other tropical regions (Guan et al., 2015), rare ground data demonstrated warming rates of +0.21 and 0.25°C per decade, respectively at Yangambi in the Democratic Republic of Congo for the period 1960-2020 (Kasongo Yakusu et al., 2023) and at Lopé in Gabon for the period 1984-2018 (Bush et al., 2020). Projections for Central Africa indicate that dry seasons will become increasingly longer, with fewer rainy days that are, however, more intense (Diedhiou et al., 2018; Fotso-Nguemo et al., 2019). Temperatures are also expected to rise, with more frequent and prolonged heatwaves (Diedhiou et al., 2018; Sullivan et al., 2020). These changes will have ecological implications, particularly for the viability of forests, which rely heavily on consistent water availability. They will face increasing stress due to both the lengthening of dry seasons and higher water demand linked to rising temperatures (Bush et al., 2019).

1.3. Tree stem growth as an indicator of environmental response

To understand the different behaviours of trees and how they respond to environmental factors, several types of measurements are possible. Among them, radial stem growth appears to be a particularly interesting measure (Wagner et al., 2014). It provides valuable information about tree physiology and their responses to environmental factors (Zweifel, 2015).

Radial stem growth results from cambial processes, which include cell division, cell enlargement, cell wall thickening, and lignification These processes are directly influenced by environmental and soil conditions such as temperature, precipitation, and soil water availability (Fan et al., 2019; Kaewmano et al., 2022). Radial stem growth is therefore a key indicator for Central African forests, as seasonality there is primarily driven by these environmental factors, as previously mentioned.

Moreover, studying growth dynamics is also an important indicator of carbon dynamics as it reflects wood formation, which is the main biological reservoir for long-term carbon sequestration (Cuny et al., 2015).

Currently, the development of automatic dendrometers, which provide high-precision data, allows for detailed measurements of radial stem growth (De Swaef et al., 2015). These instruments can detect changes with sub-micrometre precision and offer temporal resolutions ranging from 15 minutes to several years. This makes it possible to identify tree growth patterns, link them to environmental characteristics, highlight intra- and interspecific differences, better understand overall ecosystem dynamics, and relate observations to climate projections to draw conclusions about future trends (De Swaef et al., 2015; Plavcová et al., 2025; Zhou et al., 2023). However, in tropical environments, knowledge on this subject is still very limited (Plavcová et al., 2025).

All these reasons make radial stem growth a highly valuable trait for understanding how Central African forests function, both at the individual and ecosystem levels. This trait will be even more relevant in a study that combines it with leaf and canopy phenological observations, whether through remote sensing or automated observation systems. (Silvestro et al., 2025).

In this study, we focus specifically on irreversible radial stem growth and its seasonal dynamics, as measured by high-resolution automatic dendrometers. This enables us to characterise the timing and intensity of wood formation processes, and to explore

their relationship with environmental conditions. These measurements form the basis for the specific objectives outlined in the following section.

1.4. Research objectives

The main aim of this thesis is to better understand the seasonality of wood growth in canopy trees within Central African forests. By combining dendrometer data with phenological and climatic information, the study seeks to gain deeper insights into the rhythmicity of wood growth and how it is influenced by environmental factors. This work focuses on data from the Luki Biosphere Reserve (DRC), with the goal of conducting a complete analysis that can later be applied to data from other sites.

To explore this, the study addresses three main research questions:

1) What general trends can be observed at the community level among trees classified into the identified growth patterns? Are there links between absolute growth and species identity or morphological traits (e.g. leaf habit, height, wood density, basal area)
2) What growth patterns can be identified among the monitored trees? How do these patterns differ in their dynamics, and what do they reveal about inter- and intraspecific variability? Can key growth metrics such as timing, or duration characterises differences in seasonal wood growth?
3) To what extent are these growth patterns influenced by climatic conditions? Which environmental variables are most strongly associated with growth, and how might future climatic changes affect these dynamics?

As a complementary step, the study also models the average growth trajectory of highly seasonal trees using a hierarchical Gompertz model. This modelling aims to estimate the inflection date and maximum growth rate and their alignment with the climatic seasonality.

This research forms part of the CANOPi project (“Central African Network of Observatories of troPIcal”), jointly coordinated by the University of Liège and Ghent University. The project aims to assess the resilience of Central African forests in the context of climate change and increasing aridification. As part of this initiative, dendrometers and phenological cameras (phenocams) were installed at three study

sites: the Luki Biosphere Reserve (DRC), Lopé National Park (Gabon), and Okala National Park (Gabon). This thesis makes use of the data collected from dendrometers installed at Luki.

2. Material and methods

2.1. Study site

The Luki Biosphere Reserve, which spans between latitudes 5°30’ - 5°45’S and longitudes 13°7’ - 13°45’E is located in the southwest of the Democratic Republic of the Congo (DRC), in the province of Kongo Central at approximately 120 km of the atlantic coast (Ilondea et al., 2019). Covering an area of 33 000 ha, the reserve is representative of the Mayombe forest (Lubini, 1997). Its location, at the south of the Guinean-Congolese forest massif, places it on the border between the regional centre of Guinean-Congolese endemism and the Guinean-Congolese/Zambezian regional transition zone (F. White, 1983).

In terms of ecological conditions, the reserve lies almost entirely within the catchment area of the Luki River. The soils are mostly ferralitic and acidic (Sénéchal et al., 1989). According to the Köppen classification, the climate is tropical wet (Aw) (Peer et al., 2007). The forest present is referred to as "moist Central African" by Fayolle et al. (2014), corresponding to semi-deciduous forests (F. White, 1983). The reserve is home to at least 1,050 plant species, among which the most dominant trees belong to the families Meliaceae, Fabaceae, and Arecaceae (Bienu et al., 2023).

Due to its proximity to the Atlantic Ocean, the climate of the Luki Biosphere Reserve is highly influenced by ocean currents. From the south, the cold Benguela Current, which flows along the west coast of Africa, and the south-eastern trade winds play a major role. The reserve experiences a marked dry season between June and September, with monthly precipitation levels dropping below 10 mm. The rainy season lasts from October to May, although it can be interrupted by a short dry season between December and February (Couralet et al., 2013). The annual average rainfall ranges between 1150 and 1500mm (Opelele Omeno et al., 2021). As for temperatures, the monthly average ranges between 15°C and 23°C, with a mean of 19°C.

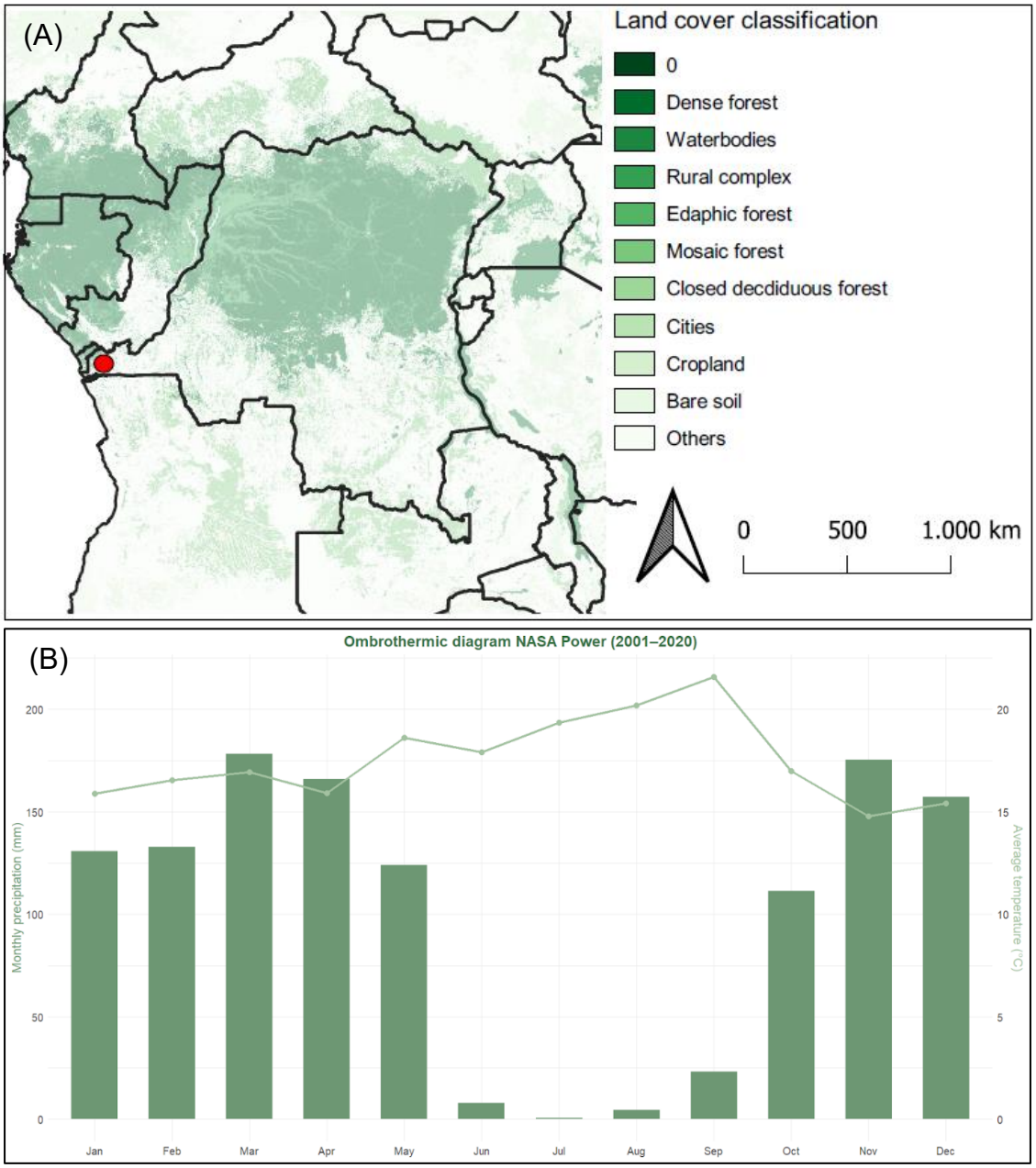

Figure 2.1: (A)The study site: Luki Biosphere Reserve (UNESCO MAB located by a red dot. The background map is the land cover classification from the Digital Earth Africa platform. (B) Ombrothermic diagrams (data from NASA POWER platform) of the study site.

2.2. Data collection

The data used in this work come from the dendrometer network installed in April 2023 by Kaddouri Marjane as part of the CANOPi project. The dendrometers are automatic TOMST point dendrometers (figure 2.2), meaning they measure tree increment at a single precise point, with a resolution below 1 µm. Another important characteristic of

these dendrometers is that they allow measurements every 15 minutes, providing high temporal resolution. Coupled with good autonomy and memory, this enables the collection of a vast amount of data in an autonomous manner. One of their main advantages is their low cost, which makes it possible to study large numbers of individuals at a broader scale. However, the dendrometers have a maximum span of 8,890 µm, which requires regular monitoring to avoid reaching this limit. Ignoring this constraint may result in data loss. This issue will be discussed in more detail later in the document

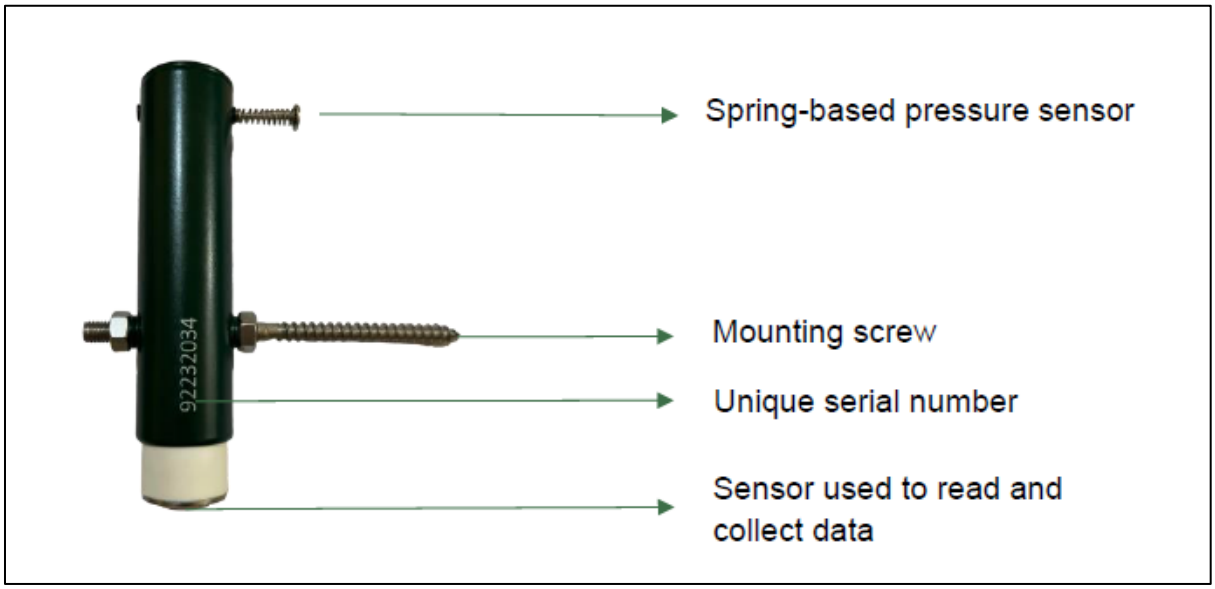

Figure 2.2: Scheme of a TOMST point dendrometer

The Luki Biosphere Reserve contain 59 dendrometers for 56 trees, as 3 of them have 2 dendrometers each. The selected trees are canopy trees in the field of views of phenological cameras installed to monitor the leaf phenology of each individual. (figure 2.3). However, these leaf phenology data are not used in this study, which focuses exclusively on the dendrometers.

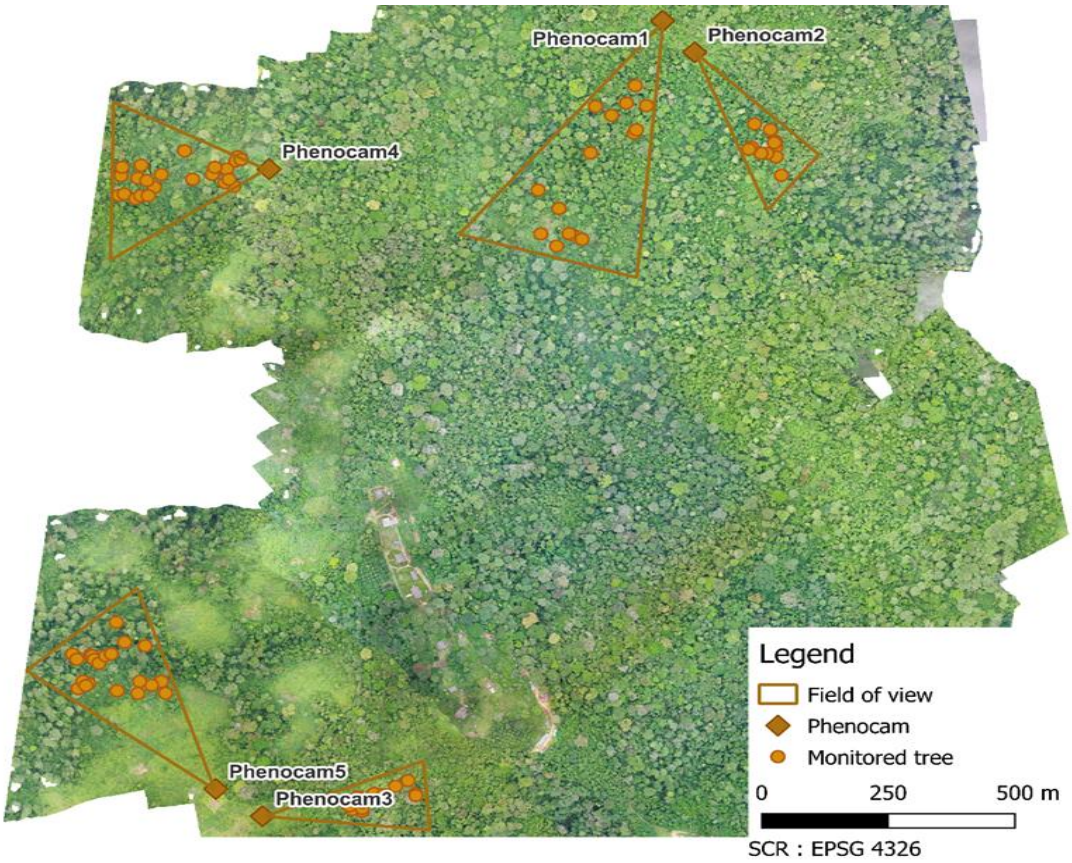

Figure 2.3: Orthophoto acquired by drone, showing the locations of the different phenocams and the trees equipped with dendrometers in the Luki Biosphere Reserve.

Data are collected every 2 or 3 months by field agents at the different sites. Given the high frequency of measurements and the number of sensors installed, a substantial volume of data has been accumulated. This makes data cleaning and preprocessing a crucial step before any meaningful analysis can be carried out.

2.3. Data cleaning

Given that measurements are taken every 15 minutes, such high temporal resolution is not required for the objective of this study. Therefore, only one measurement per day was retained. However, it is important to take into account that trees show hourly stem radius variations in three distinct phases: growth, shrinkage, and swelling (figure 2.4). Luse et al. (2024) showed that most trees enter the growth phase at sunset and reach their maximum increment rate between 6 a.m. and 9 a.m. in the Luki Biosphere Reserve. Consequently, this time window was chosen for daily measurement extraction. During field data collection, when the sensor comes into contact with the dendrometer, a small spike is observed in the signal due to its high sensitivity. The daily measurement retained in this study was taken at 6 a.m., just before field agents start their working day at 7 a.m.

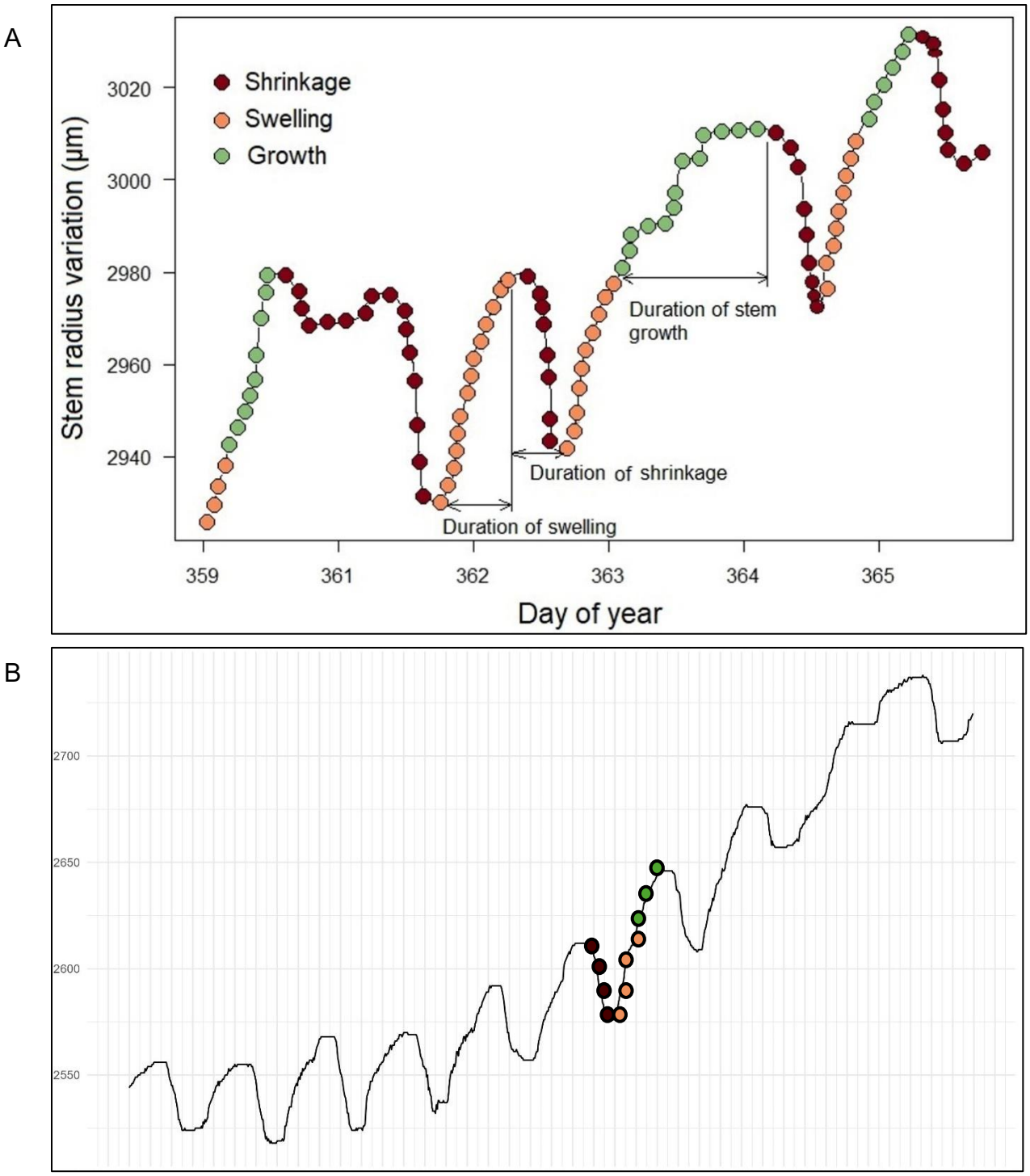

Figure 2.4: (A) The three distinct phases of the stem radius variation: growth (green), shrinkage (red) and swelling (orange) (Luse et al. 2024). (B) Zoom on the growth period (between 10 and 19 April 2024) of a tree (92232071 – Dialium pachyphyllum) showing these three distinct phases represented with same legend as in panel A.

To ensure the reliability of daily measurements, correction procedures were applied to account for artefacts, such as dendrometer calibration when the maximum span was reached (loosened screws causing large negative jumps), and positive spikes induced during field data collection. Calibration jumps (figure 2.5A) were corrected by adjusting the curve after each detected event, while fieldwork-induced spikes (figure 2.5B) were

smoothed using a LOESS trend curve (span = 0.3) within a 100-day window and replacing values over a 15-day interval around each collection date. Finally, a 7-day moving average was applied to reduce residual noise, yielding cleaned data ready for analysis (figure 2.5C).

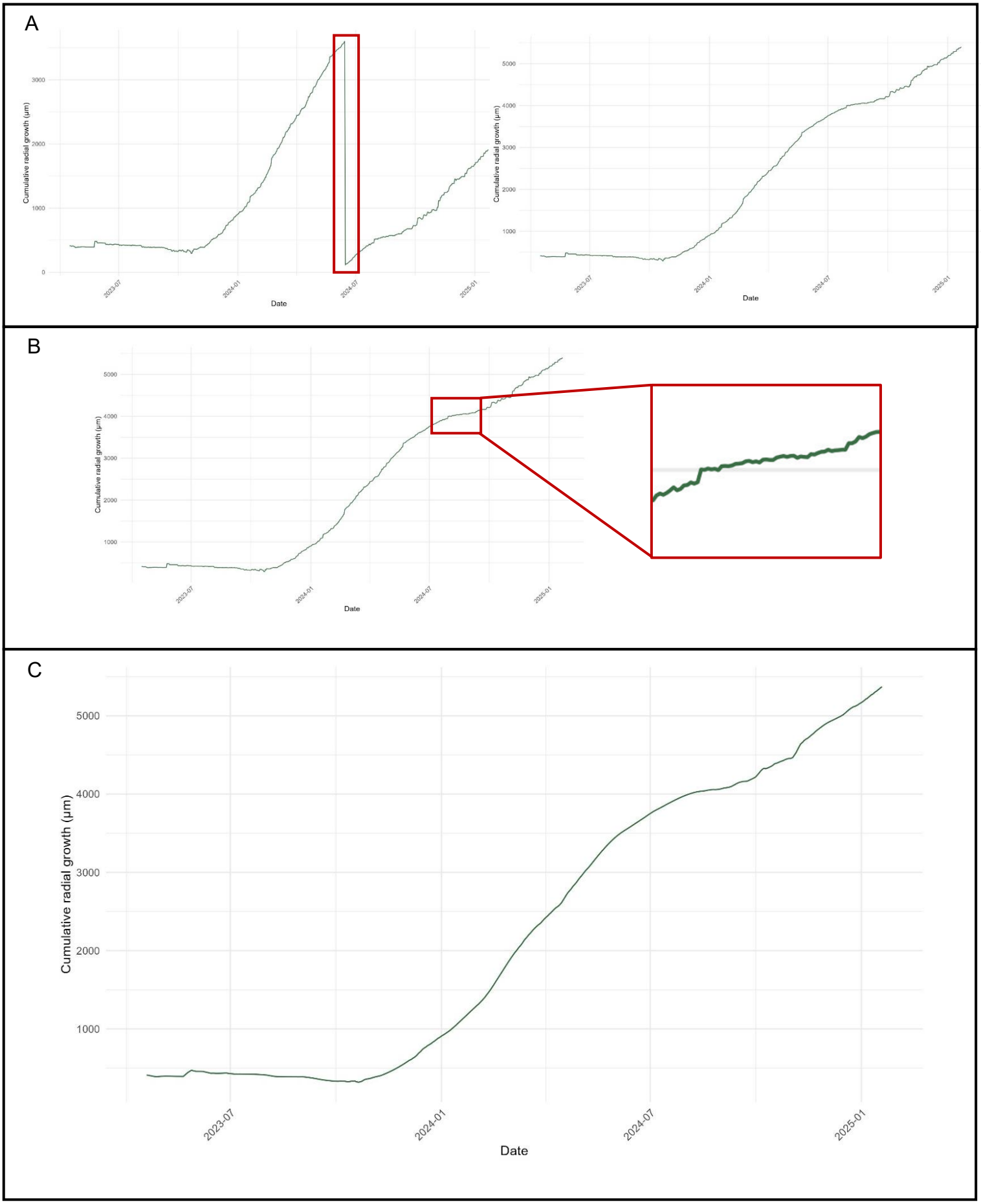

Figure 2.5: Data cleaning framework on a tree (dendrometer 92232071 – Dialium pachyphyllum):(A) Big negative jumps due to recalibration cleaning framed in red and the same cumulative radial growth curve without the jump, (B) illustration of a minor discontinuity resulting from field data collection operations and (C) cleaned cumulative radial growth curve.

Finally, some limitations had to be acknowledged regarding the dataset used in this study. First, some dendrometers (3 dendrometers out of 59) were excluded from the analysis because they were installed to replace previous devices that had been damaged or stolen. The period between the end of measurements and the installation of the replacement was too long, resulting in a significant loss of information. The new dendrometers will be analysed once they have collected enough data. Another limitation was related to unexpectedly rapid growth in some trees. Several dendrometers were close to reaching their maximum range of 8890 µm, and some unfortunately reached it (see in appendix, figure A1), which resulted in a loss of data and required their exclusion from the study (5 dendrometers out of 59).

2.4. Growth patterns

An exploratory visual analysis was carried out to classify whether growth patterns could be observed in the study site. Using the time series, recurrent patterns could be identified. These observations were guided by the general shape of the curve, such as the presence of growth stagnation periods, slope fluctuations (increasing or decreasing but without stagnation), or constant or null slopes. A decision tree was created to formalise the visual reasoning involved in this work (figure 2.6).

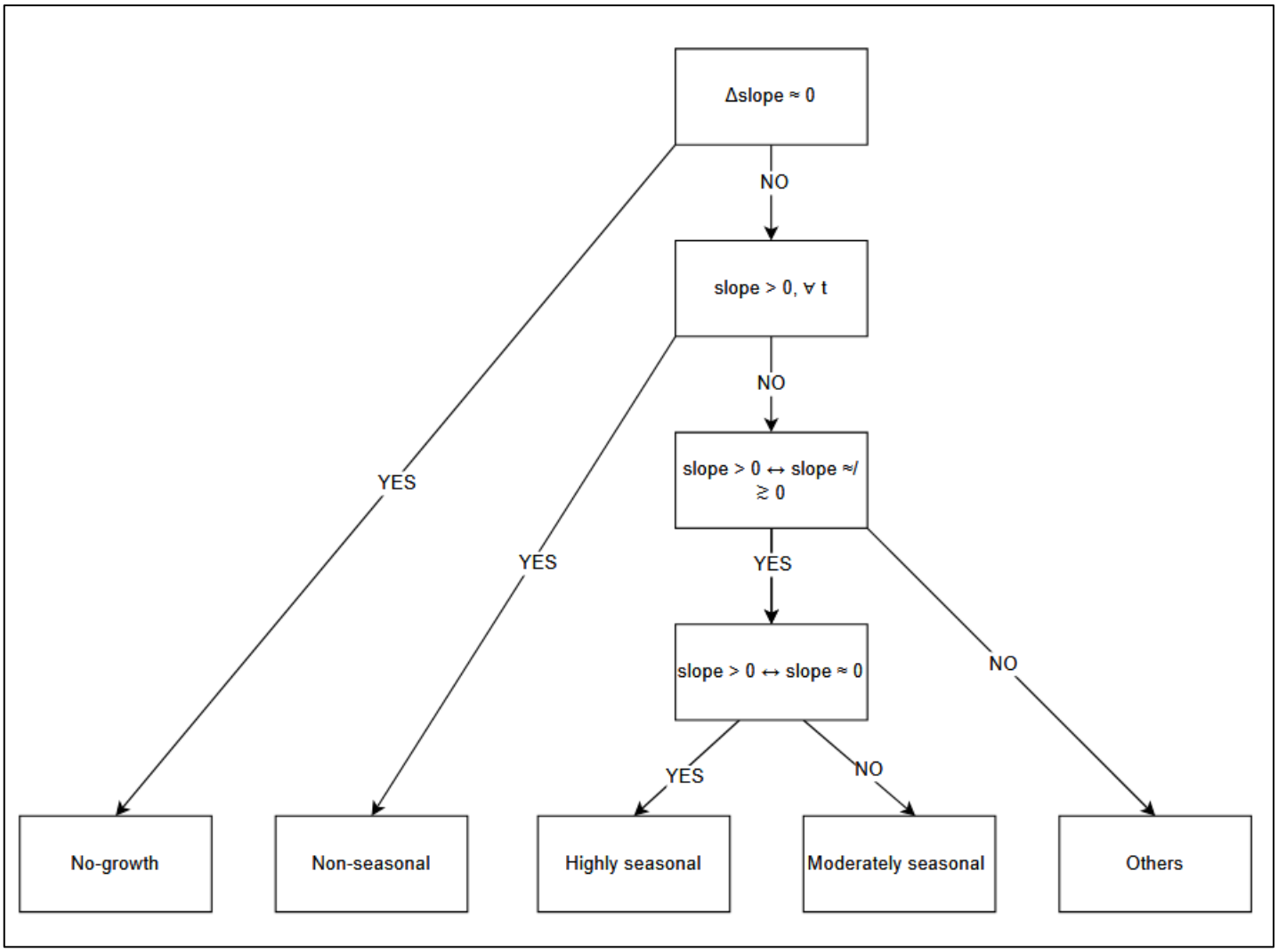

Figure 2.6: Decision tree of the visual approach developed to characterise growth patterns

This process made it possible to develop an explanatory typology of the different growth patterns, which are presented and defined in the results section. To visualise the general growth patterns, we computed the cumulative radial growth for each dendrometer over the study period. Trees were then assigned to one of four growth pattern categories highly seasonal, moderately seasonal, non-seasonal, and no-growth based on the typology developed. For each category, the cumulative growth curves of all individuals were plotted together, with colours representing the monitored species. This allows also a direct visual comparison of inter- and intra-specific variability within each growth pattern.

The trees corresponding to each pattern were grouped, a LOESS (Cleveland & Devlin, 1988) trend curve (span = 0.3) was fitted to each individual curve. The average trend of each pattern was then calculated and graphically represented along with the associated standard deviation. These patterns were also graphically represented using

boxplots for each month, allowing visualisation of the temporal dynamics of growth across the entire monitoring period. Each boxplot corresponds to the distribution of growth increments (in µm) within the group for a given month. This visualisation helped identify periods of active growth and stagnation period for each pattern. It is important to note that some trees did not show any general pattern. This deviation from the observed typology will be addressed later in this document.

Before conducting further analyses, a selection step was applied to retain only trees that clearly conformed to one of the main identified growth patterns. Trees with excessively noisy signals or atypical behaviour that did not fit the defined typology were excluded from the main analysis. These cases are not discussed in the core results due to the limited interpretability of their signal, but they are presented in appendix (figure A2) for transparency. These exclusions are also revisited in the discussion section as part of the study's limitations and perspectives.

2.5. Community-level trends

Following this filtering, a set of selected trees was retained for further exploration. First, an average trend curve will be created to determine whether, at the community scale, there is a seasonality in growth. Their characteristics including DBH, height, basal area, species, leaf habit (Gorel, 2025), wood density (Vieilledent et al., 2023; Zanne et al., 2009), pattern assignment (as defined in figure 2.6), and total absolute growth over the full monitoring period were compiled in a table presented in the results section. The heterogeneity of the community will be explored using boxplots for these different traits.

A preliminary analysis was then conducted to explore whether differences in absolute growth across the sample could be associated with morphological or categorical variables. Boxplots were used to assess differences in growth based on categorical traits (e.g. leaf habit and group classification), while scatterplots were produced to explore relationships with continuous variables (e.g. height, DBH, wood density). Statistical tests included the Wilcoxon test (for comparisons of leaf habit) (Wilcoxon, 1945) and the Kruskal–Wallis test (for group classification) (Kruskal & Wallis, 1952). These exploratory analyses aimed to identify potential structural drivers of growth

variation at the sample level, before shifting focus to the detailed analysis of growth dynamics and patterns.

2.6. Breakpoint analysis

In order to identify major changes in trends in the curves produced previously, and automatically, a breakpoint analysis (Vanoni et al., 2016) was performed. To yield more robust results, two different approaches were developed in this work.

First, a breakpoint analysis using a sliding window is performed. To identify a breakpoint, a linear regression (cumulative radial growth vs. DOY) is fitted within a 45-day window sliding forward in 7-day steps between each window, which allows a balance between robustness and sensitivity. The 25% strongest slope variations are retained to focus on more significant breakpoints. The successive changes in these slopes are then calculated, and a score combining absolute and relative variation at each candidate breakpoint is computed, allowing the detection of both major slope changes and significant breakpoints even on small slopes. Candidate breakpoints close in time are grouped, and one breakpoint from each group is retained based on the previously calculated score.

Secondly, a breakpoint analysis by structural break analysis using the RStudio package “strucchange” (Zeileis et al., 2002) is performed. More precisely, using the command “breakpoints”, the time series is split into homogeneous sub-intervals. Then, the slopes are calculated on each segment and significant changes between successive slopes are identified based on a threshold using the 75th percentile. Significant breakpoints kept have a slope change greater than the 75th percentile.

Breakpoints detected by the two approaches are combined, and a final visual analysis is performed to select the breakpoints that are ultimately kept, which allows drawing very accurate breakpoints that are then characterised as either growth acceleration breakpoints or growth stagnation breakpoints based on the difference in slope before and after each breakpoint.

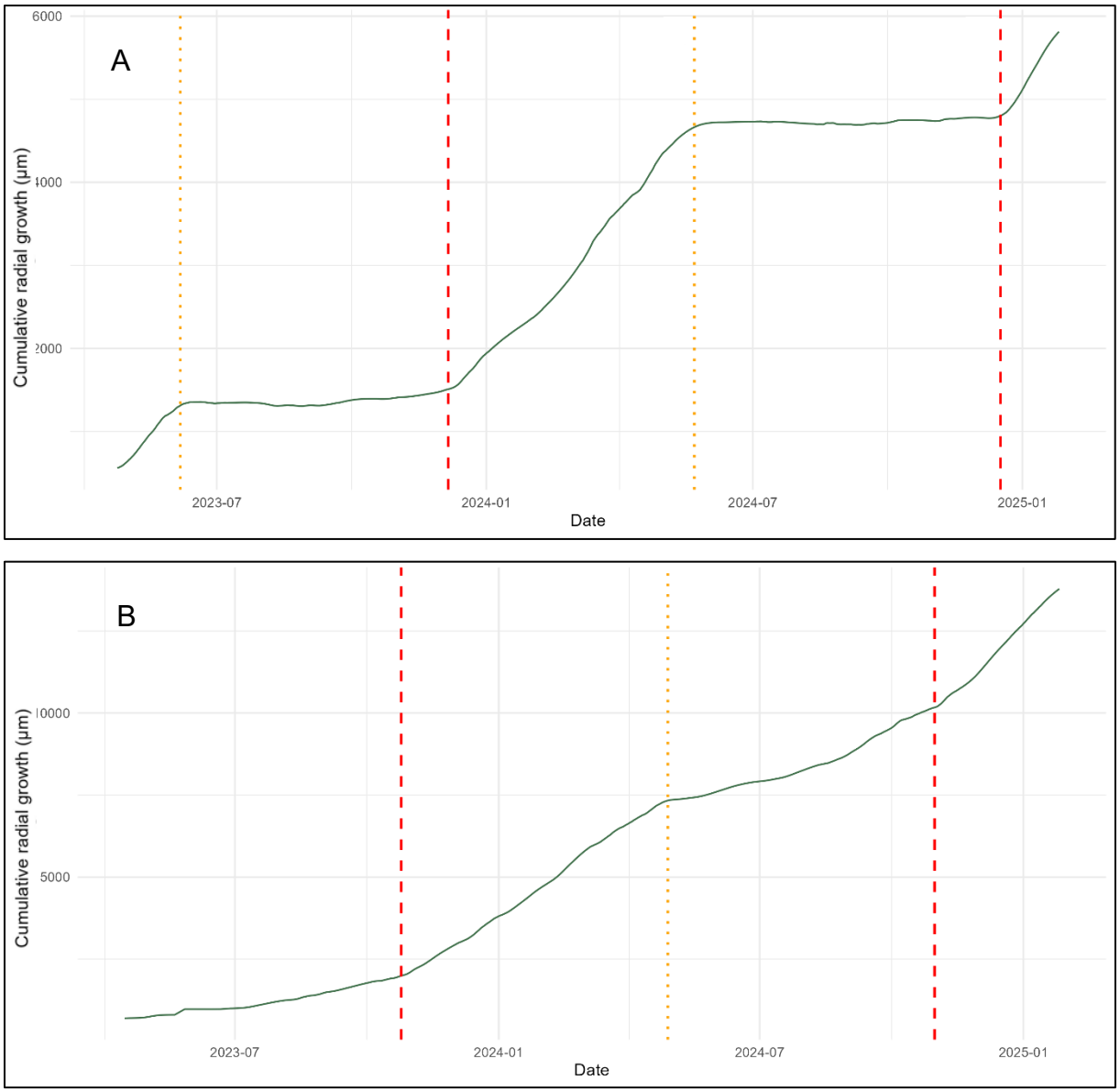

Figure 2.7: Illustration of two individuals (A: dendrometer 92232003 – Zanha golungensis (HS); B: dendrometer 92232029 – Piptadeniastrum africanum (MS)) with their selected breakpoints. Red markers indicate acceleration breakpoints, while yellow markers indicate stagnation breakpoints.

To quantify the magnitude of each validated breakpoint, the corrected time series was divided into two windows of equal duration centred on the breakpoint date (Bai & Perron, 2003). A pre-event window and a post-event window, each covering 21 days, were extracted. A simple linear regression was fitted separately to the data in each window, and the slopes of these regressions were compared. The absolute difference between the pre- and post-event slopes was then scaled to a 0–1 range using a min–max normalisation, allowing direct comparison of breakpoint strength across trees and events.

This analysis allows providing some very interesting growth parameters, such as the start and end of the growing season, the number of consecutive days of growth, and complements the various conclusions that can be drawn about the seasonality of the trees in this study.

For trees with highly or moderately seasonal growth patterns, these metrics were summarised graphically. A horizontal bar plot was produced to represent, for each tree, the estimated start and end dates of growth, with bar lengths corresponding to the number of growth days.

Finally, to assess whether morphological characteristics could help explain the distribution of trees across the identified growth patterns, an exploratory analysis was carried out. Four structural variables were considered: basal area and wood density.

Boxplots were generated to visualise the distribution of each variable within the three growth pattern categories (highly seasonal, moderately seasonal, non-seasonal). To statistically assess potential differences between groups, Kruskal–Wallis tests (Kruskal & Wallis, 1952) were performed for each trait. This non-parametric test was chosen due to the small sample sizes.

2.7. Inter- and intra-species variations

To further illustrate the inter- and intraspecific variation in growth observed throughout the analysis, a summary figure was produced. Absolute growth was plotted for each species using weighted boxplots, with individual trees shown as separate data points. This representation highlights both the distribution of growth values within species and differences between species. Where applicable, intra-individual variability is also visible for trees equipped with two dendrometers. This visual approach complements the pattern-based analysis and provides a clearer picture of growth variability at the species and individual levels.

2.8. Link between growth and environmental conditions

To explore the potential influence of environmental conditions on wood growth, a visual comparison was carried out between the mean growth trend curves for each of the three identified patterns and several climatic and hydrological variables.

A multi-layered plot was produced to align growth dynamics with daily values of precipitation (mm), air temperature (°C), vapour pressure deficit (VPD, hPa), relative humidity (%), and net surface radiation (MJ/m²). Additionally, volumetric soil water content (m³/m³) was extracted at multiple depths to examine potential differences in water availability and uptake over the course of the growing season. While ERA5 provides valuable continuous coverage, particularly in data-scarce tropical regions, it is important to acknowledge that satellite-derived soil moisture estimates may exhibit biases under dense forest canopies and are known to underestimate absolute values in such contexts (Muñoz-Sabater et al., 2021; Yang et al., 2022). However, relative changes over time are still considered reliable for identifying trends and seasonal transitions.

These visual analyses were used to identify the timing of growth onset and cessation in relation to environmental changes, and to detect potential lags or thresholds in response, especially regarding rainfall and soil moisture. Particular attention was paid to contrasting responses between the three growth pattern groups.

In addition to the visual time-aligned analyses, a complementary correlation analysis was performed to quantify the relationship between daily radial growth and environmental variables. Monthly means were computed for both daily growth increment and climate variables across the three years of monitoring. These included air temperature, precipitation, VPD, relative humidity, net surface radiation, and volumetric soil water content at four depth intervals (0–7 cm, 7–28 cm, 28–100 cm, 100–255 cm).

The Pearson correlation coefficient was calculated between daily radial growth increments and each environmental variable. The results were displayed in a multi-panel plot, where each point represents a correlation for a given year and each line tracks the monthly trend. Dashed lines were added to indicate the average timing of

growth onset (red) and cessation (blue), allowing visual alignment with seasonal trends in climate and growth.

2.9. Gompertz modelling

To characterise the average growth trajectory, hierarchical Gompertz models (Zeide, 1993) were fitted exclusively to the highly seasonal growth pattern. This restriction was motivated by the requirement for an alternation of stagnation and acceleration phases in order to capture the S-shaped form of the Gompertz function. Only individuals assigned to the highly seasonal group within a common global time window (from 1 August 2023 to 1 August 2024) were retained. For each dendrometer series, data were resampled at three temporal resolutions (weekly, biweekly, and monthly) by averaging corrected cumulative radial growth measurements within fixed intervals. Values were then scaled to a relative growth percentage between 0 and 100%. Time was normalised between 0 and 1 within the selected window. All individual series belonging to the highly seasonal pattern were then combined into a single dataset for model fitting, allowing the fixed effects to represent the mean trajectory of the entire pattern, while the random effects captured individual deviations.

For each resolution, a hierarchical non-linear mixed-effects Gompertz model was fitted, with individual dendrometers as the grouping factor. The parameters μ (growth rate) and λ (relative timing of the inflection point) were included as fixed effects representing the mean growth trajectory for the pattern, while random intercepts for μ and λ accounted for between-tree variability. Model fitting was performed using the nlme package in R (Pinheiro et al., 1999). To stabilise estimation and ensure that parameter values remained within their biologically meaningful ranges, μ was log-transformed so that its estimates, when back-transformed, were strictly positive, while λ was logit-transformed so that its back-transformed values remained constrained between 0 and 1.

The modelling procedure was applied at two levels: to all individuals assigned to the highly seasonal pattern to obtain the overall pattern trajectory, and separately to all individuals of each species within this pattern to assess species-specific growth trajectories. For each model, fixed-effect estimates were used to generate the mean curve, and the corresponding variance-covariance matrix (Kümmel et al., 2018) was

used in parametric simulations to generate 500 plausible sets of parameters. This procedure preserves both the uncertainty in each parameter and their correlation structure, ensuring realistic combinations of μ and λ. The simulated curves were then used to compute confidence intervals. The root-mean-square error (RMSE) between the mean curve and the observed mean growth values per date was computed as a measure of model fit, and the inflection date was obtained from λ scaled to the global date window. In addition, the onset and cessation of growth were defined as the dates when the fitted curve reached 5% and 95% of its total amplitude, respectively, providing a consistent and model-based estimate of the growing season.

Although models were initially fitted at three temporal resolutions (weekly, biweekly, and monthly), only the biweekly resolution was retained for subsequent analyses. This decision was based on a compromise between temporal detail and data smoothing.

3. Results

3.1. Community-level trends

The cumulative radial growth of the entire cleaned dataset was first analysed at the community scale. This exploratory analysis was conducted by grouping trees according to the growth typology developed in this study, distinguishing three categories: highly seasonal (HS), moderately seasonal (MS), and non-seasonal (NS). Figure 3.1 presents the average trend curve of all dendrometers retained in the study, along with the associated standard deviation. As shown in the boxplots (see in appendix, figure A3) trees following a highly seasonal pattern dominate the overall signal, accounting for 46% of the total basal area (12 trees out of 26). However, periods of stagnation in the average curve are not entirely flat due to the influence of the other growth types: moderately seasonal (24%, 5 trees out of 26) and non-seasonal (30%, 9 trees out of 26), which contribute to the overall shape of the composite.

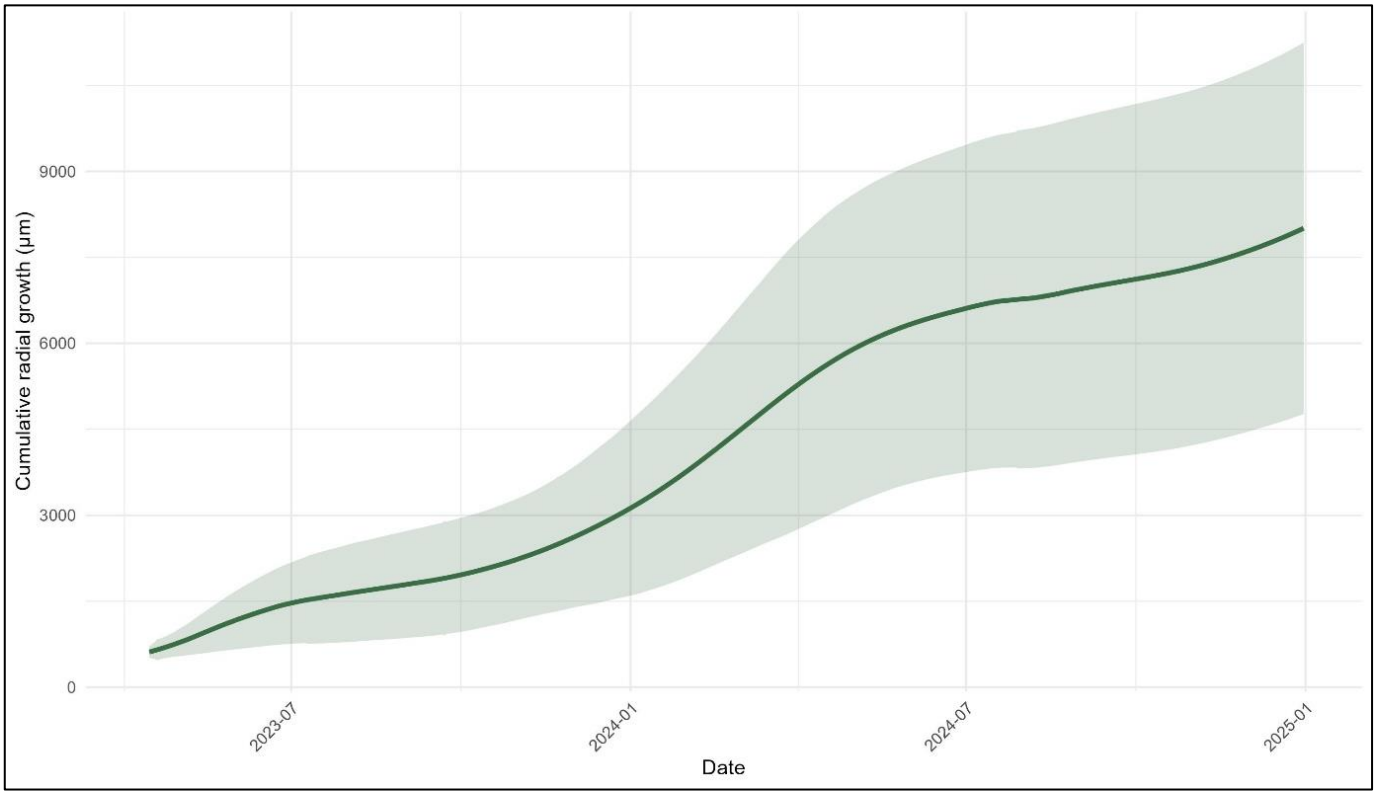

Figure 3.1: Mean trend growth curve with associated standard deviation, illustrating the overall growth dynamics among the 26 trees retained in the study.

The table in appendix (table A1) provides an overview of these trees, including their structural characteristics (e.g. DBH, height, basal area), species identity, leaf habit, group assignment (see figure 2.6), and total absolute growth over the full monitoring

period. The dendrometer ID of each tree is also included. The boxplots (figure 3.2) indicate that, within the community, there is substantial variability among individuals, both in their structural characteristics and in their absolute growth. Absolute growth varied widely across the sample, with a mean value of 7,850 µm and a standard deviation of 3,270 µm over a period of 20 months.

Figure 3.2: Distributions of basal area (m²), wood density (g/cm³) and absolute growth (µm) in the studied community. Boxes show the median, interquartile range and extremes. Scales differ by variable.

To explore whether this variability might be explained by tree-level traits, boxplots and scatterplots were produced to examine relationships between absolute growth and both categorical (e.g. leaf habit, group classification) and continuous variables (e.g. height, DBH, wood density). Statistical tests were applied to assess whether growth differed significantly between categories. The associated figures are presented in the appendix section (figure A3 and A4).

Firstly (see in appendix, figure A3a), the highly seasonal pattern is the most represented among the trees, but it displays a lower median absolute growth compared to the other categories. However, the Kruskal–Wallis test yielded a p-value above 0.05, indicating that the observed differences in absolute growth between the pattern groups are not statistically significant.

Regarding leaf habit (see in appendix, figure A3b), deciduous trees are more frequent in the sample, but the Wilcoxon test also indicated no significant difference in absolute growth between deciduous and evergreen species.

The scatterplots (see in appendix, figure A4) exploring the relationships between absolute growth and continuous morphological traits (height, DBH, wood density) show a high degree of dispersion, with no clear associations emerging.

Taken together, these results suggest that none of the traits examined here provide a satisfactory explanation for the observed variability in absolute growth over the monitoring period. This highlights the need to focus on growth dynamics within defined wood growth patterns.

3.2. Wood growth patterns

One of the key results of this study is the identification of four distinct wood growth patterns among the monitored trees, based on the general shape of their smoothed growth curves. I define following four different general growth patterns among the individuals:

- Highly seasonal: growth curves show alternating periods of growth and stagnation, with increment values close to zero (12 trees, belonging to 7 species).
- Moderately seasonal: growth curves show alternating periods of growth acceleration and slowdown, without ever reaching values close to zero (5 trees, belonging to 4 species).
- Non-seasonal: growth curves display slopes that remain mostly positive throughout the year (9 trees, belonging to 9 species).
- No-growth: the growth curve displays a flat slope, indicating no detectable growth. Only one individual falls into this category and will therefore not be shown (1 tree, belonging to 1 species).

In figure 3.3, the curves retained following the classification are shown for each of the presented patterns. It can be noted that, in addition to being the only representative of trees showing no growth, data recording for this tree was stopped due to an accident. The newly installed dendrometer has not yet collected enough data to be presented.

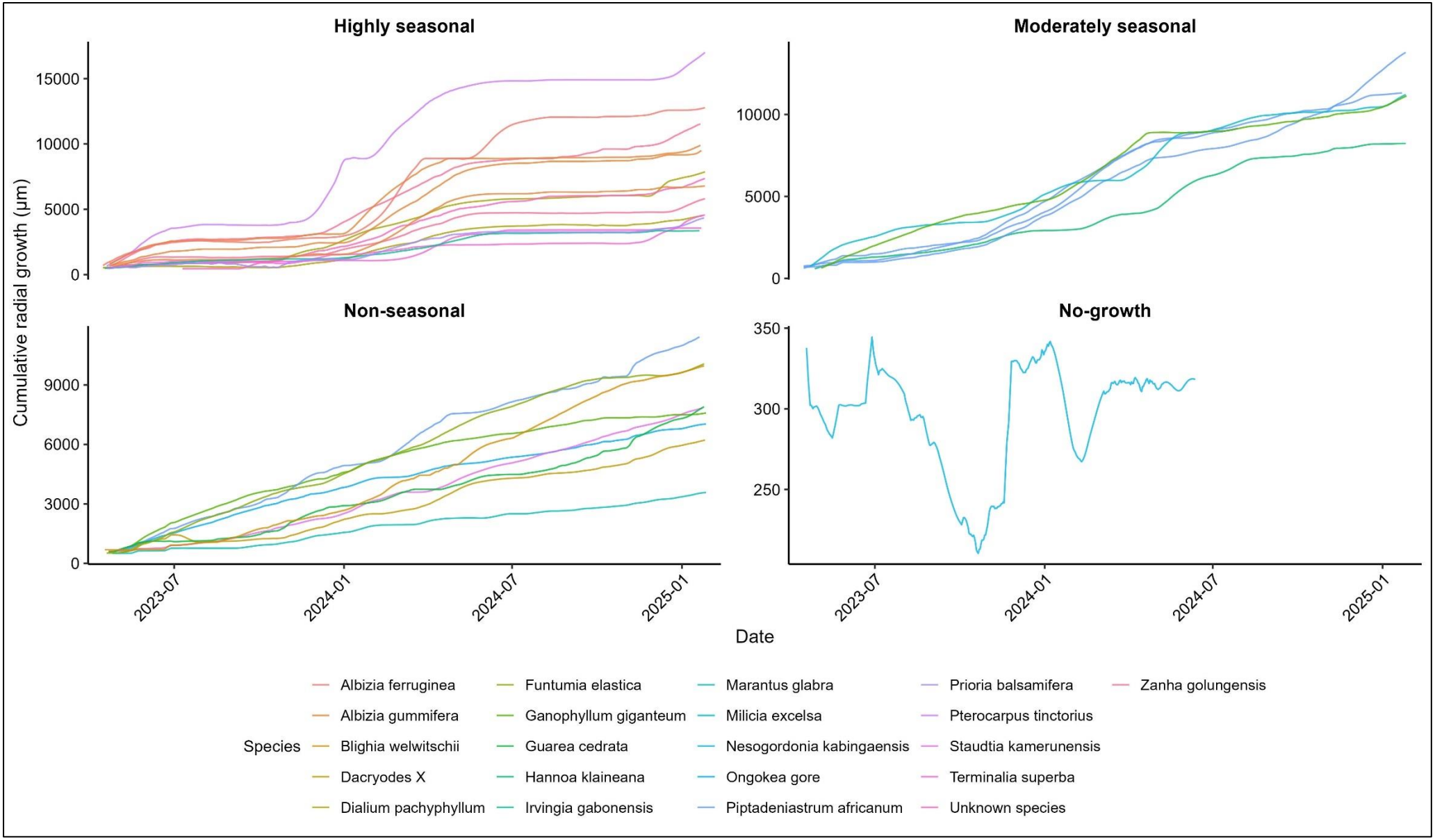

Figure 3.3: Cumulative radial growth (µm) of monitored trees grouped into four growth patterns: highly seasonal (top left), moderately seasonal (topright), non-seasonal (bottom left), and no-growth (bottom right). Each line represents the smoothed growth curve of an individual tree, colour-coded by species.

In figure 3.4, the three general growth patterns are illustrated (highly seasonal (a), moderately seasonal (b), and non-seasonal (c)) using the mean trend curve with the associated standard deviation (left panels) and the corresponding monthly increment boxplots (right panels). Each mean trend curve confirms the definitions previously described. Indeed, one can clearly observe the alternations between periods of growth and stagnation in the highly seasonal pattern (a), alternating accelerations and slowdowns in growth in the moderately seasonal pattern (b), and finally a nearly constant slope in the non-seasonal pattern (c). The standard deviation of each trend curve also shows that all individuals used to construct the trend follow the same general pattern, but there is considerable variation in growth intensity between trees. For the highly seasonal and moderately seasonal patterns, a periodic trend can be observed, with stagnation events typically occurring around June and growth events around November. The monthly increment boxplots confirm these general patterns: stagnation periods, with increments close to zero, are observed for the highly seasonal pattern; slowdown periods appear as decreasing increments that do not reach zero; and increments remain relatively constant for the non-seasonal pattern. The considerable variation in growth between trees and the periodic nature of the previously described events of growth and stagnation or slowdown are also highlighted by these boxplots.

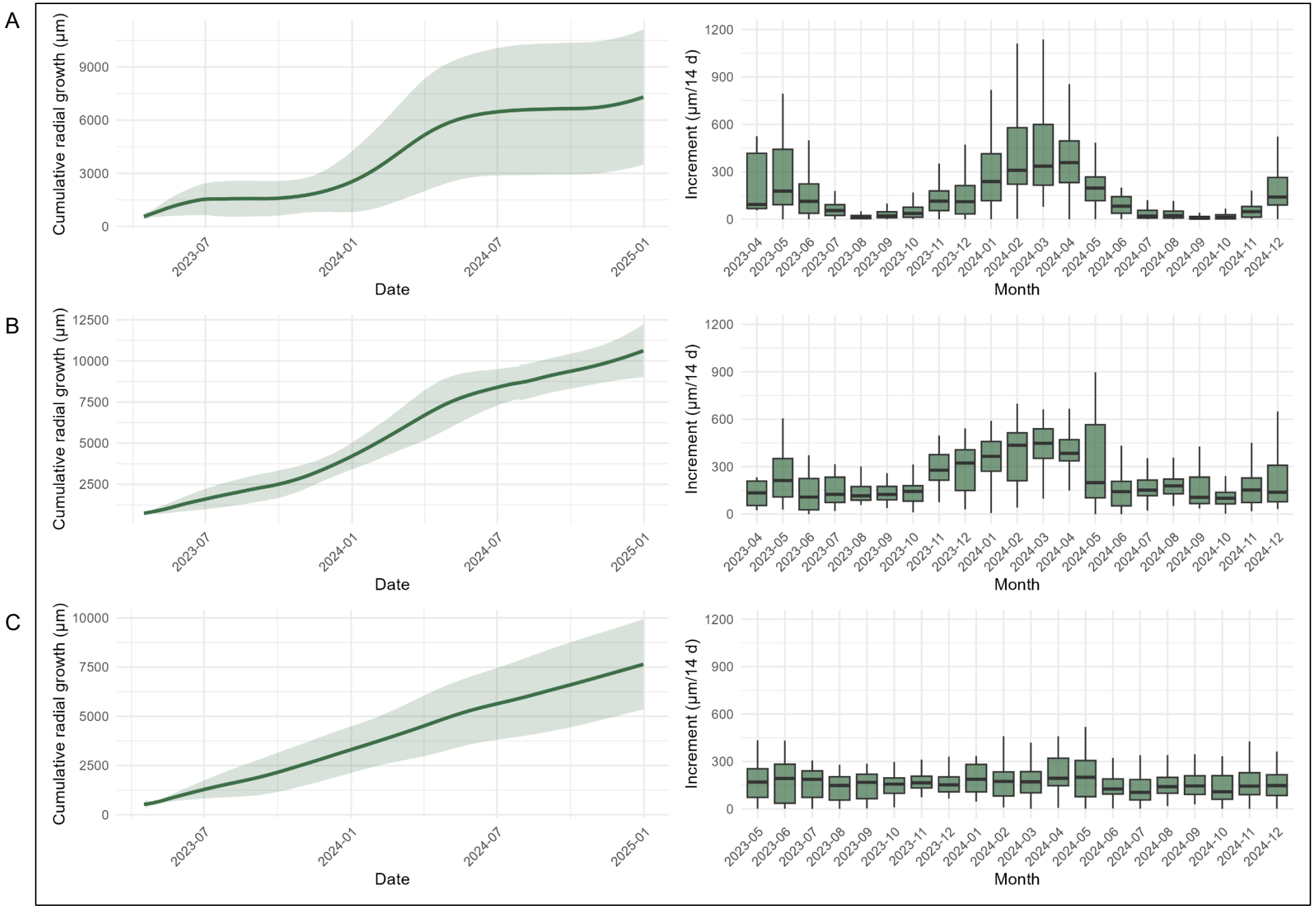

Figure 3.4: Mean cumulative radial growth (left) and monthly increments (µm/14 days aggregated per month) (right) for the three identified growth patterns: A = highly seasonal, B = moderately seasonal, C = non-seasonal. Green lines show LOESS trends (span = 0.3) with standard deviation in shading; boxplots display monthly increment distributions.

3.3. Breakpoint analysis

The metrics derived from the breakpoint analysis performed on each tree in the three general growth patterns are summarised in three tables available in appendix, one for each pattern. Based on the available data, a complete growth period for the first two patterns is observed between August 2023 and August 2024. The following analysis will therefore focus on this period for trees classified as highly seasonal and moderately seasonal. Before presenting the metrics, a breakpoint scoring was carried out to validate both the algorithm and the visual selection developed in this study, to verify the accuracy of the method. Table in appendix (table A2) presents the average performance values of the breakpoints detected for each dendrometer, as well as the number of detected breakpoints, and the minimum and maximum performance values. The results show that the average performance values are consistently high (at least 0.8), which supports the conclusion that the developed method is accurate.

a) Highly seasonal

The highly seasonal (detailed metrics in appendix, table A3) group has an average growing season of 158 ± 35 days. It is also the most represented growth pattern in our dataset, accounting for 46% of the total monitored basal area. Growth onset ranges from DOY 250 in 2023 to DOY 47 in 2024 (mid-October to late February), reflecting substantial variability. In contrast, the onset of the stagnation phase marking the end of the growth period occurs within a narrower window, from DOY 91 to 190 (late March to late June). Consequently, the number of growth days varies widely, from 112 to 243, suggesting that the triggers for growth cessation are likely more limiting.

Growth rate spans from 8.74 to 66.57 µm/day, and absolute growth also varies strongly, supporting the hypothesis of marked interspecific variability. Intraspecific variability is present but noticeably lower. Apart from two *Dialium pachyphyllum* individuals, all trees in this group are deciduous, pointing to a strong link between leaf habit and growth pattern. The most represented family is Fabaceae. Finally, two trees equipped with paired dendrometers (* and **) show differences in growth onset, cessation, season length, absolute growth, and thus growth rate, possibly reflecting non-uniform radial growth around the stem. Figure 3.5 examines whether season length influences absolute growth.

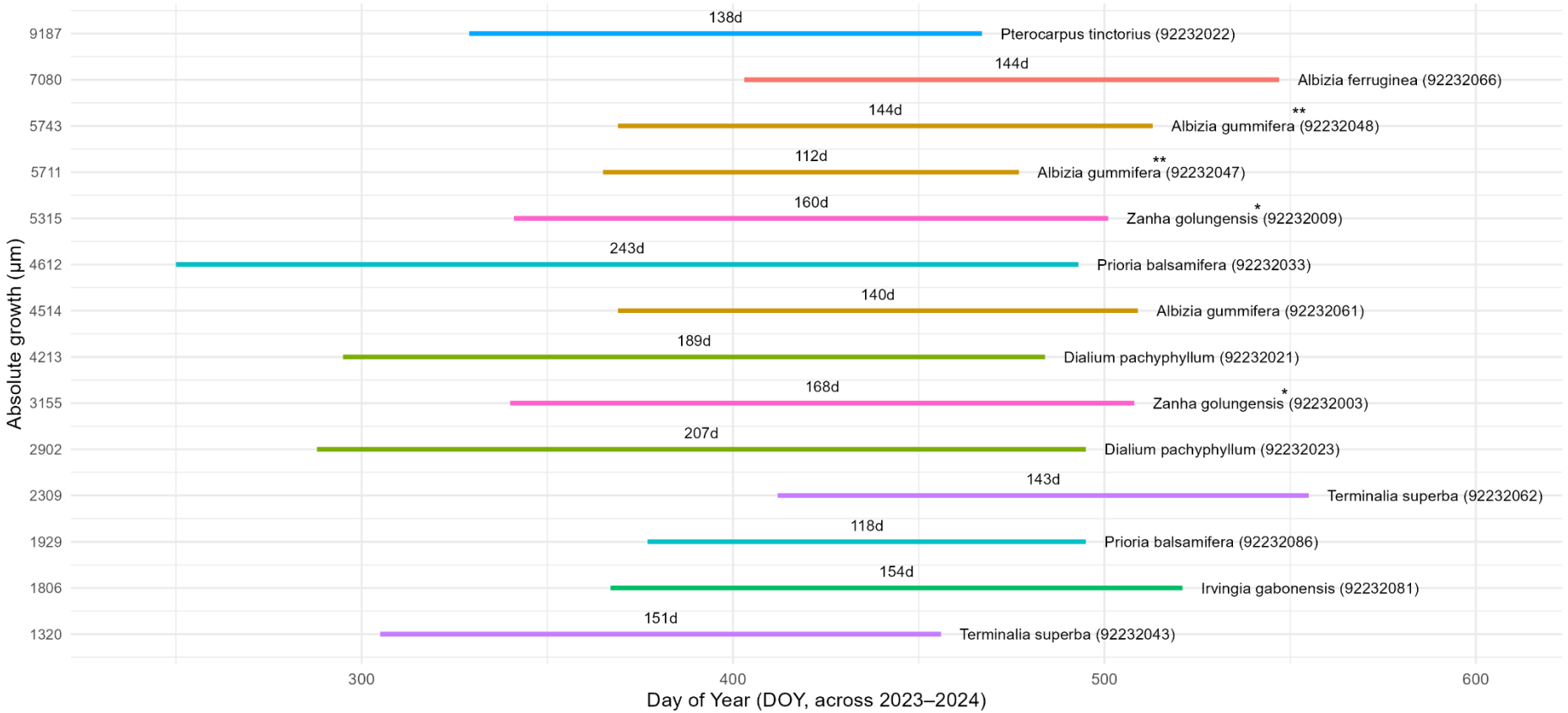

Figure 3.5: Growth periods of trees with a Highly Seasonal pattern, sorted by total absolute growth. Each horizontal line represents the duration of the growth phase between the start and end day of year (DOY), with the number of growth days indicated above the line. Species names and dendrometer IDs are displayed at the end of each line. The DOY axis spans from August 2023 to August 2024, with 2024 DOYs adjusted by +365 for continuity. The Y-axis indicates the total absolute growth (µm) over the growth period.

Figure 3.5 first highlights that the number of growth days does not clearly influence absolute growth during the studied period. It also confirms the earlier observation that the growth cessation occurs within a narrower time window than the start, further suggesting the presence of a factor strongly controlling growth cessation. This points towards the timing of growth potentially being more important. It is plausible that climatic conditions play a significant role and should be taken into consideration.

b) Moderately seasonal

The moderately seasonal (detailed metrics in appendix, table A4) group has an average growing season of 180 ± 36 days. Growth onset occurs between DOY 303 in 2023 and DOY 38 in 2024 (mid-October to late February). The slowdown phase generally begins between DOY 112 and 148, with one notable exception: *Hannoa klaineana*, which enters stagnation unusually early, at DOY 229. Excluding this outlier, variability in the timing of both growth acceleration and deceleration remains low, resulting in a relatively narrow range in the number of growth days (110 to 210).

Most trees in this group are deciduous, although conclusions should be drawn cautiously given the small number of individuals. *Piptadenastrum africanum*, equipped with two dendrometers (***), shows highly consistent values across all metrics. In this pattern, both growth rate (GR) and absolute growth vary much less than in the Highly Seasonal group, suggesting a potential link between growth period length and absolute growth, as further examined in Figure 3.6.

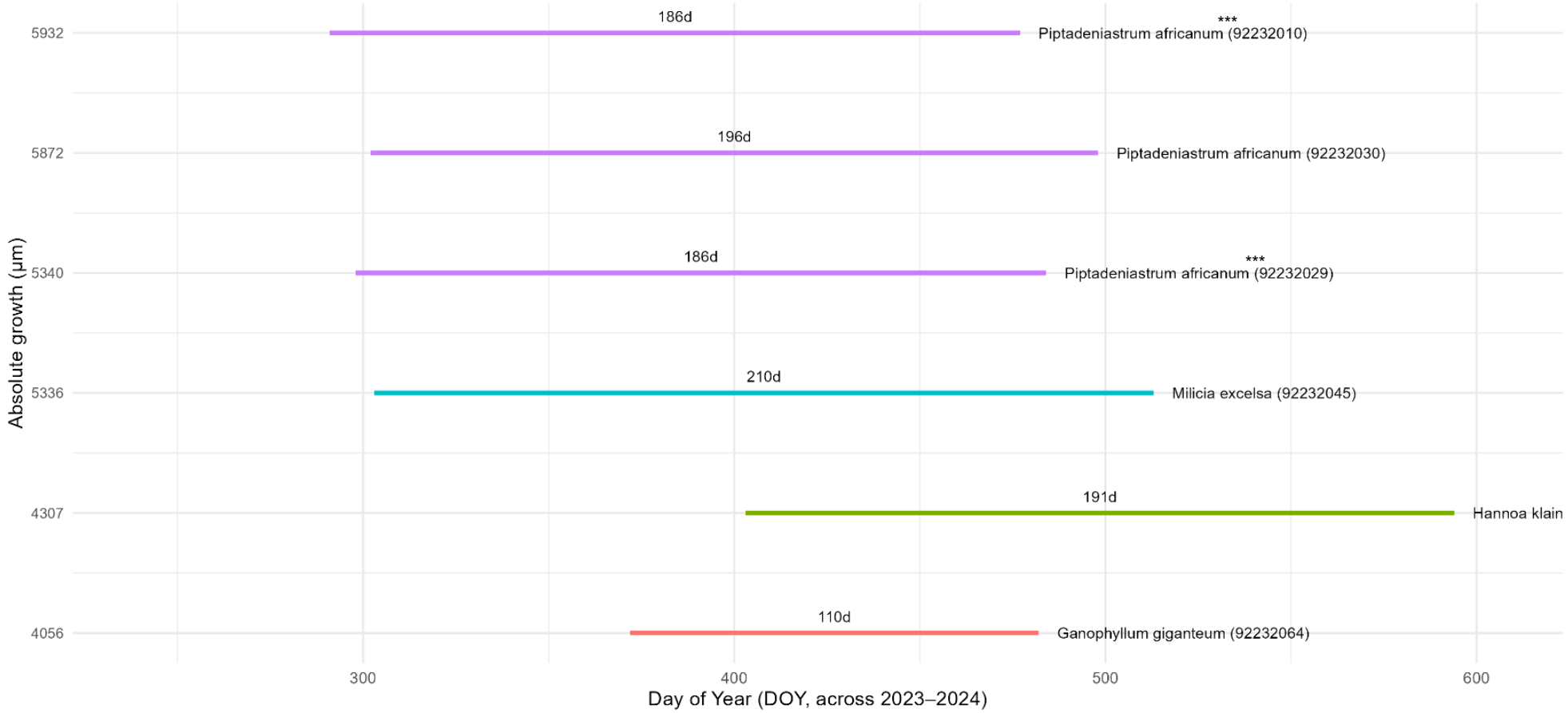

Figure 3.6: Growth periods of trees with a moderately seasonal pattern, sorted by total absolute growth. Each horizontal line represents the duration of the growth phase between the start and end day of year (DOY), with the number of growth days indicated above the line. Species names and dendrometer IDs are displayed at the end of each line. The DOY axis spans from August 2023 to August 2024, with 2024 DOYs adjusted by +365 for continuity. The Y-axis indicates the total absolute growth (µm) over the growth period.

Figure 3.6 above shows a clear relationship between absolute growth and the duration of the growth period, in contrast to the highly seasonal pattern. The offset observed for *Hannoa klaineana* is also clearly visible and remains difficult to explain. This case would warrant further investigation, either by including more individuals or by extending the study period to better understand its growth behaviour. The case of *Piptadeniastrum africanum* is also of interest, as they appear to be fairly synchronous. This may be explained partly by the fact that two of the three dendrometers are installed on the same tree, and also because they are located within the same study site.

It can be hypothesised that, in this pattern, the trees are less sensitive to external factors, especially given that their growth does not fully stop, unlike in the previous category.

c) Non-seasonal

The non-seasonal group consists of trees for which no breakpoint was detected, with detailed metrics available in appendix (table A5). Several individuals displayed continuous growth throughout the study period, with growth rates ranging from 4.74 to 16.98 µm/day. Most of these rates are lower than those observed during the growth phases of the other two patterns. This group also shows strong interspecific variability, but the limited data do not allow conclusions to be drawn regarding intraspecific variability. A notable feature is the high proportion of evergreen species, in clear contrast with the other patterns. Based on their overall trend, individuals in this group appear to be less influenced by external factors, maintaining steady growth throughout the year.

Based on the previous results, we were already able to draw several conclusions regarding the parameters that define the different growth patterns. These include the overall shape of the growth curves, the alternation between growth/stagnation or acceleration/deceleration phase or the absence of such alternation as well as the leaf habits of the corresponding individuals. It is therefore relevant to explore whether morphological traits can also determine the pattern to which a tree belongs. Figure 3.7 presents boxplots showing the distribution of the basal area and wood density. A Kruskal-Wallis test was performed to assess whether significant differences exist between the distributions. The results show that none of the tests were significant (p-

values > 0.05), suggesting that morphological characteristics do not allow the different growth patterns to be distinguished.

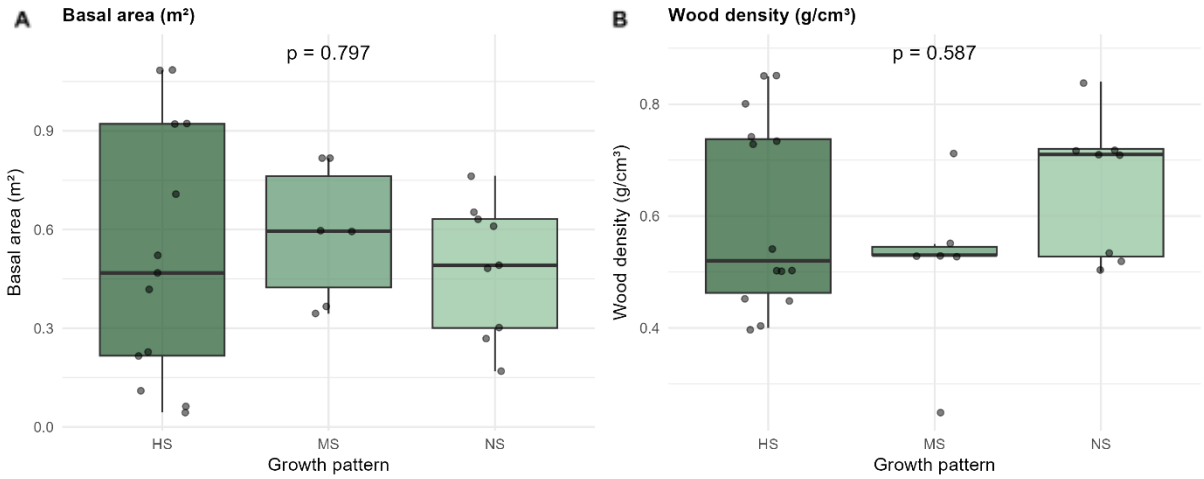

Figure 3.7: Boxplots showing the distribution of two tree traits: basal area (m²) (A), and wood density (B) (g/cm³) across the three growth pattern categories: Highly Seasonal (HS), Moderately Seasonal (MS), and Non-Seasonal (NS). Individual points represent tree-level measurements. The Kruskal-Wallis p-values, shown above each plot, indicate whether trait distributions significantly differ among the groups.

3.4. Inter- and intra-specific variations

The results presented in the previous sections already highlight considerable variability in growth patterns, both between and within species. These differences were reflected in morphological traits, leaf habits, absolute growth, and the pattern classifications.

To complement these observations, figure 3.8 presents absolute growth across all studied species. Each boxplot represents a species, with individual trees shown as points. For species represented by multiple individuals, intraspecific variability is clearly visible. In some cases, growth values vary widely between individuals of the same species, suggesting a potential influence of microenvironmental or physiological factors.

This figure provides a synthetic view of inter- and intraspecific variation in absolute growth and reinforces earlier findings. It also highlights that even species with few individuals can display strong internal variability, and in some cases, individual trees equipped with two dendrometers showed noticeable intra-individual differences.

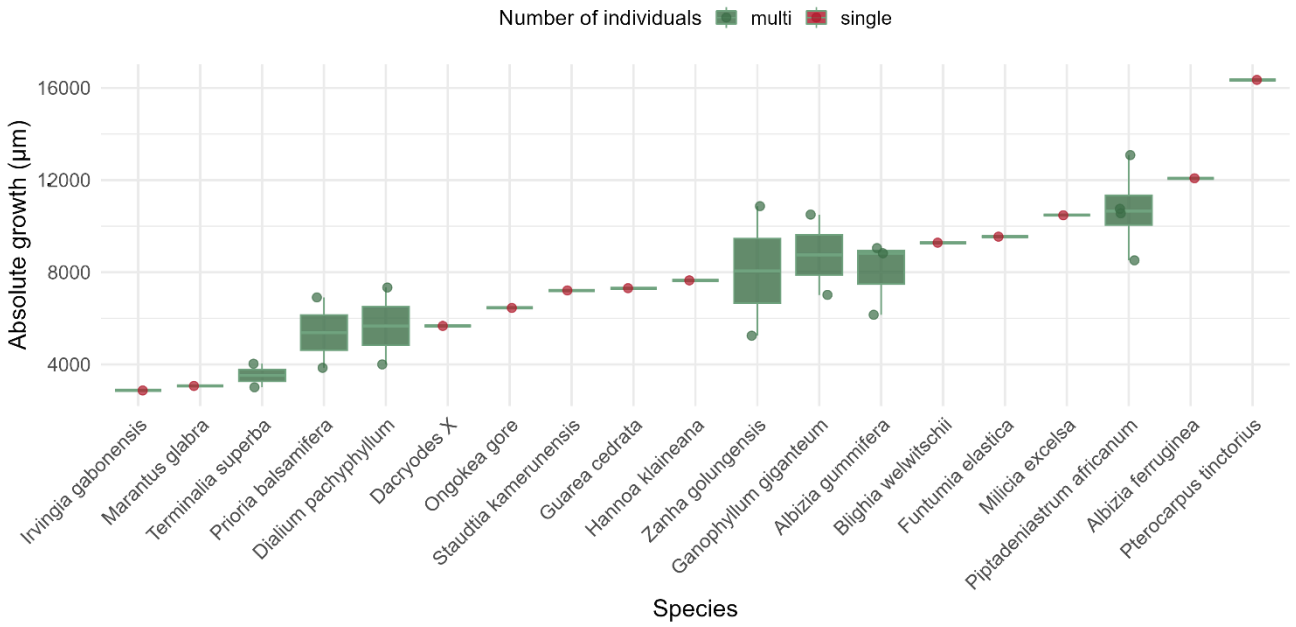

Figure 3.8: Boxplots show the distribution of absolute growth for each species, with individual measurements represented as points. This visualisation highlights both the variability among species and the range of growth responses within species

3.5. Link between growth and environmental conditions

To investigate the influence of environmental conditions on wood growth, the figures below compare the mean growth trend curves for each of the three identified patterns with a range of climatic and hydrological variables. The figure 3.9 shows the evolution of air temperature, vapour pressure deficit (VPD), net surface radiation, relative humidity (RH), daily precipitation, and volumetric soil water content at four depths, from the surface layer (0–7 cm) to the deepest one (100–255 cm) aligned with growth trends.

For trees classified as highly or moderately seasonal, a consistent pattern emerges. The onset of growth (highlighted by the first red dashed line) closely coincides with the beginning of the rainy season and is accompanied by an increase in temperature, VPD, and radiation. Interestingly, growth tends to begin only after a clear accumulation of soil water across all layers, suggesting the existence of a moisture threshold that must be reached before growth resumes. This may also explain the variability in the timing of growth onset between trees.

Growth cessation (marked by the second red dashed line) appears more synchronised and occurs shortly after the end of the rainy season. It is associated with declining values in all key climatic variables and a progressive decrease in soil moisture, especially at greater depths, where active water uptake is visible. This supports the

earlier observation that growth cessation is more tightly controlled than initiation, possibly due to a limiting environmental factor.

By contrast, trees with a non-seasonal growth pattern show little to no alignment with the investigated environmental parameters, suggesting a different mode of regulation or lower climatic sensitivity.

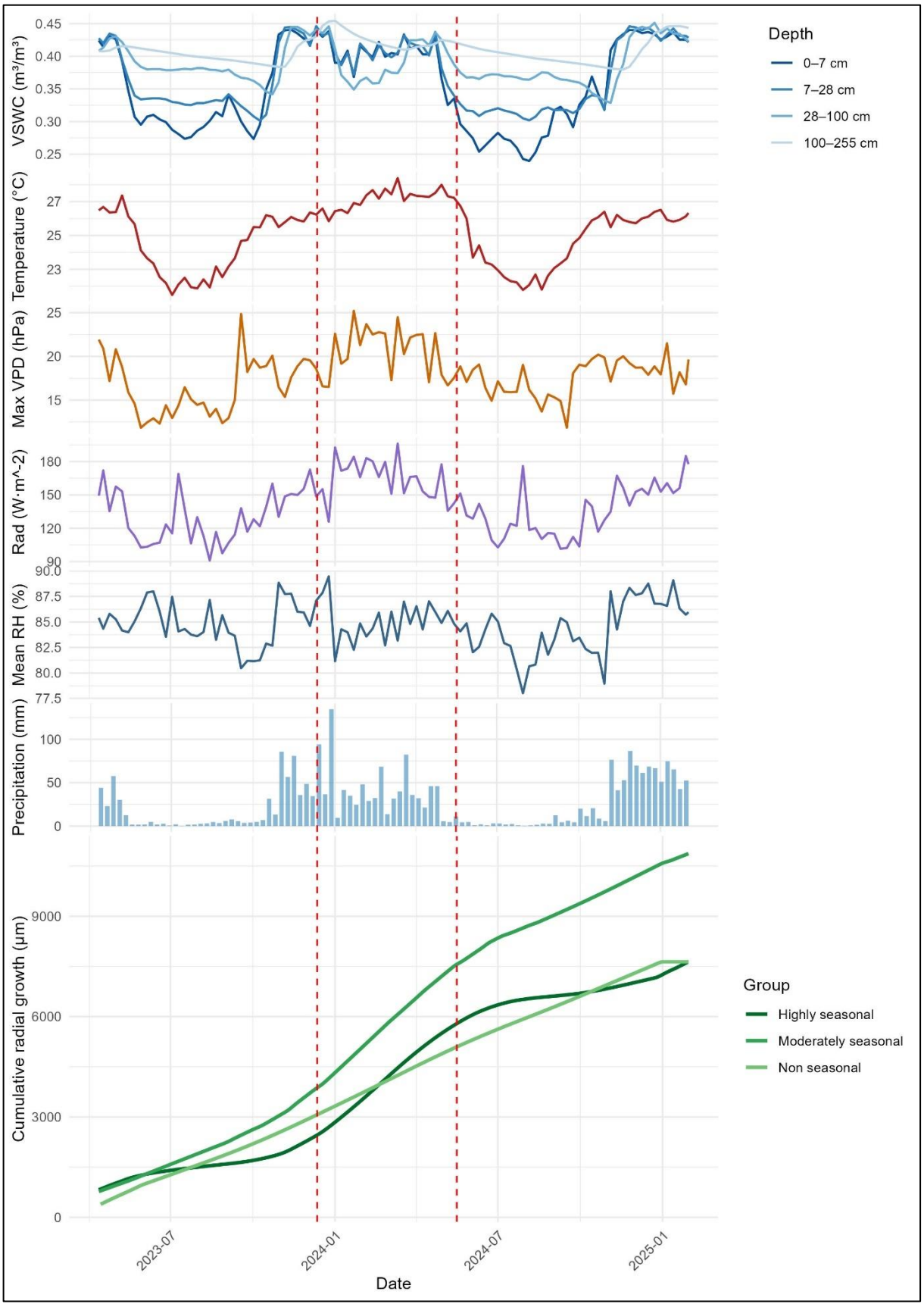

Figure 3.9: Multi-layered plot showing the relationship between the mean trend curve of the three patterns and various environmental variables. Precipitation (mm), relative humidity (RH, %), net surface radiation (W/m²), maximum VPD (hPa), temperature (°C) and volumetric soil water content (VSWC; m³/m³) at different depths (0–7 cm, 7–28 cm, 28–100 cm, and 100–255 cm). Environmental data were extracted from the ERA5 database.

To complement the time-aligned visual analyses, a correlation analysis was performed between daily growth increments and a range of climatic and soil variables, using monthly mean values aggregated across the three monitored years. Figure 3.10 presents the Pearson correlation coefficients obtained for each variable, with separate lines representing the temporal evolution of correlations over the year. The red dashed line indicates the average timing of growth onset for the seasonal patterns.

Overall, the clearest and most consistent relationships are found between growth and water-related variables, particularly precipitation and volumetric soil water content across all four depth layers. These correlations tend to strengthen around the onset of the growing season, confirming the key role of increasing water availability in triggering growth resumption.

In contrast, environmental variables such as temperature, radiation, VPD, and relative humidity exhibit more variable or weaker correlations with growth.

Importantly, trees classified as non-seasonal show much weaker and less consistent correlations across all variables, supporting the idea that their growth is less linked to external climatic cues.

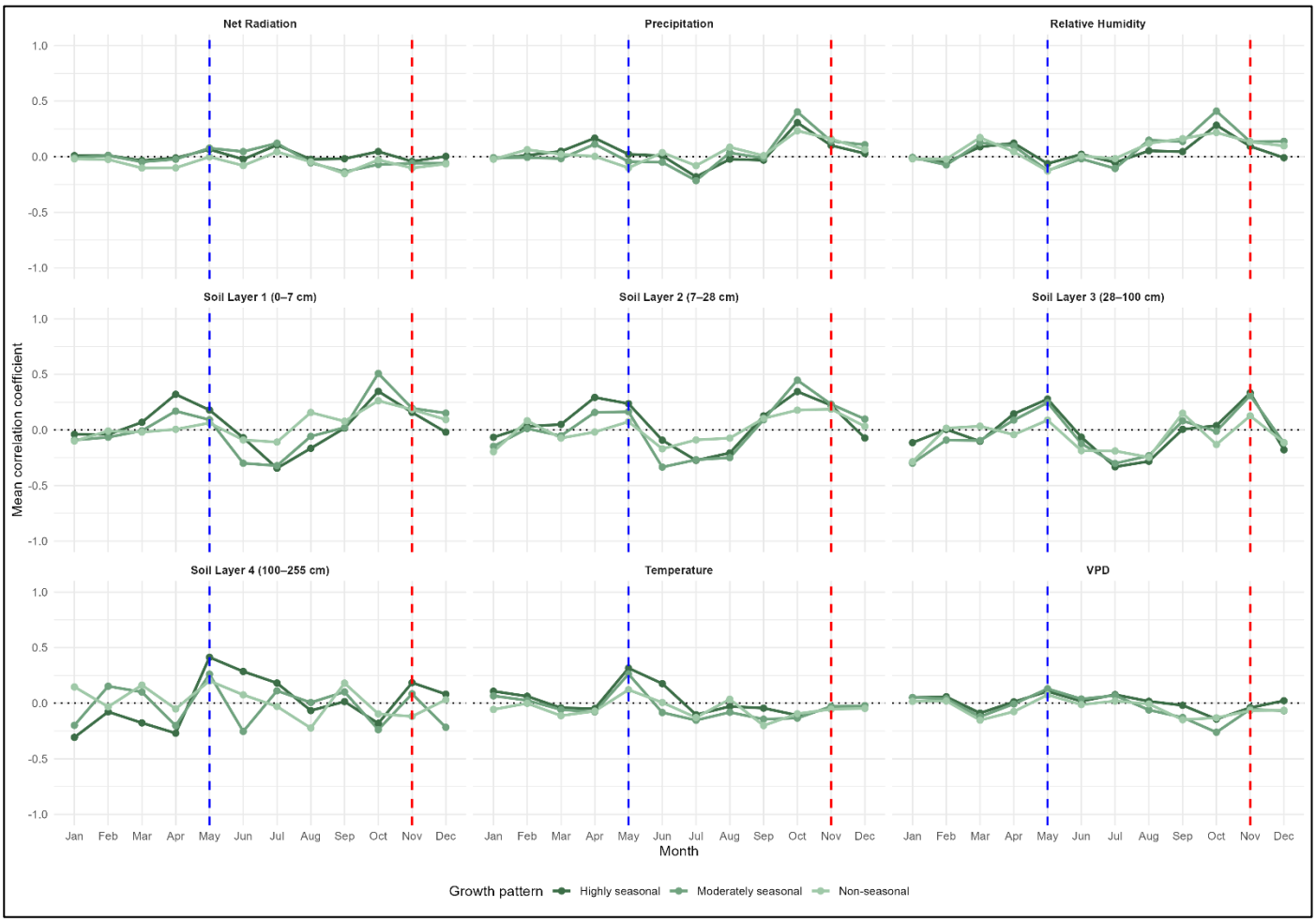

Figure 3.10: Monthly correlations between average growth of the different patterns and key environmental variables. Each panel shows the Pearson correlation coefficient between monthly growth and a given environmental variable, calculated for each year of monitoring. Variables include net radiation (W/m²), total precipitation (mm), relative humidity (%), volumetric soil water content (VSWC) at different depths (0–7 cm, 7–28 cm, 28–100 cm, 100–255 cm), air temperature (°C), and vapour pressure deficit (VPD, hPa). Red dashed lines indicate the beginning of the main growth period and blue dashed lines indicate the end of the period.

3.6. Gompertz modelling

A Gompertz model was fitted within the highly seasonal pattern, focusing on the complete growth period identified in this study (from 01/08/2023 to 01/08/2024) (figure 3.11), as well as at the species level for each species present in this pattern, as shown in appendix (figure A5).

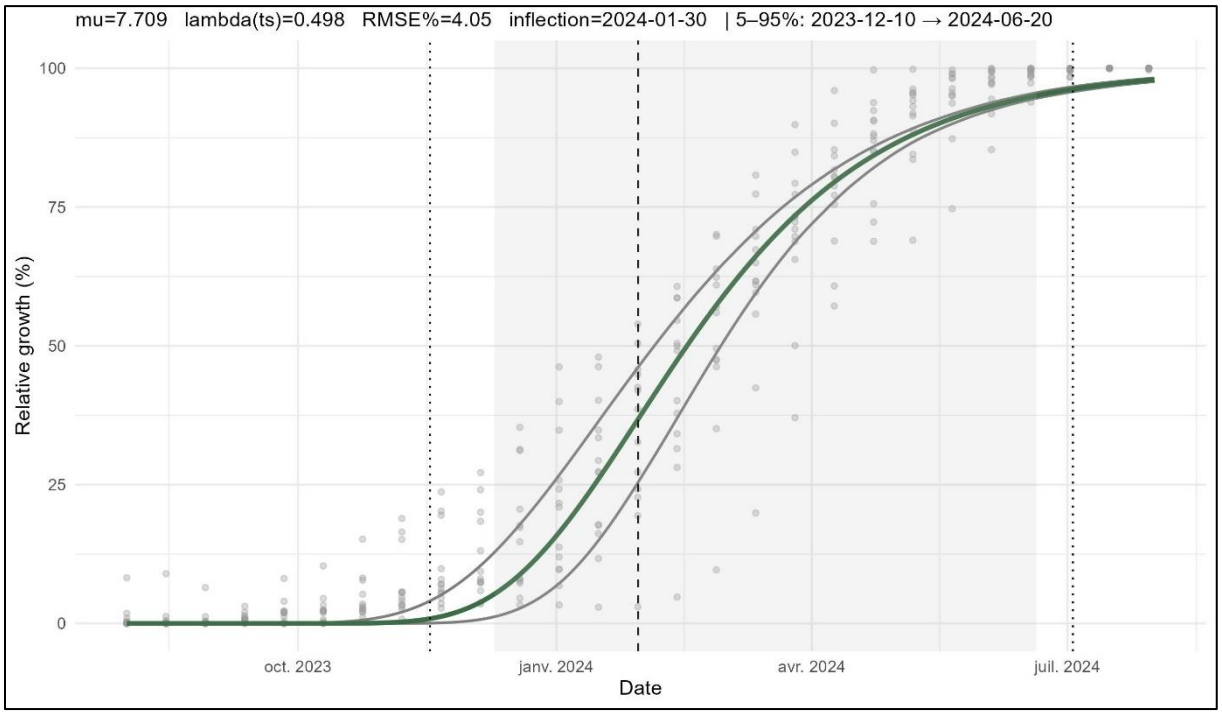

Figure 3.11: Hierarchical Gompertz fit (green) with confidence bands (grey) for highly seasonal trees (biweekly data). Grey dots: individual dendrometer measurements (relative growth, %). Vertical dashed line: inflection point; shaded area: 5–95% growth period.

It can immediately be noted that the model fits well, as indicated by the low RMSE% (4.05%). Another noteworthy point is the inflection date, reached on 30 January 2024, with the maximum growth rate occurring around this point. After this date, the growth rate begins to decrease, although growth remains sustained. When examining the models for individual species, this inflection point consistently occurs between January and February, except for *Terminalia superba*. Considering the variability in growth onset highlighted in figure 3.5, it appears that the growth slowdown occurs regardless of the start date of the growth period. It is also evident that this inflection point takes place just after the monthly maximum in precipitation and before the monthly minimum in the rain season (figures 3.9), potentially corresponding to the short dry season that can be observed between December and February (Couralet et al., 2013). This

observation further supports the idea that precipitation plays an important role in sustaining growth.

In addition, the Gompertz model identified the overall growth phase as occurring between mid-December and mid-June. These results are consistent with the breakpoint analysis performed for this pattern.

4. Discussion and perspectives

The aim of this study was to enhance our understanding of the seasonal dynamics of wood growth in canopy trees from Central African forests. Using dendrometer data from the Luki Biosphere Reserve, combined with environmental and phenological records, we addressed three main research questions: identifying community-level growth trends and their links to species traits, describing and comparing seasonal growth patterns and their variability, and assessing the influence of climatic and environmental factors on these dynamics.

The discussion follows these three axes and integrates a complementary Gompertz modelling analysis (figure 3.11) to provide quantitative insights into the timing and trajectory of seasonal growth. This approach ensures alignment with the initial research framework while allowing for a progressive interpretation from community-level observations to broader environmental influences and ecological implications.

4.1. Community-level growth trends

The first research question aimed to identify general wood growth trends at the community level and to explore potential links with morphological and functional traits. At this scale, a clear growth seasonality was observed (figure 3.1), largely driven by the predominance of seasonal and deciduous trees. This morphological trait is indicative of seasonal growth, marked by an alternation of growth and stagnation periods, directly associated with the loss and onset of foliage (Angoboy Ilondea et al., 2021)

Absolute growth was then analysed across all available data to investigate possible relationships with immutable traits such as height, wood density, basal area, and leaf habit (see in appendix, figure A3 and A4) . No significant link could be established, although this conclusion should be treated with caution due to the small sample size. In contrast, previous studies in Central Africa have shown that tree diameter influences diameter growth (Gourlet-Fleury et al., 2023; Ligot et al., 2022) and that wood density can improve models for predicting aboveground biomass, which is also associated with diameter growth (Djomo et al., 2016).

Expanding the dataset through additional dendrometer installations could provide the statistical power needed to detect such relationships. Moreover, incorporating competition-related variables, such as the basal area of neighbouring trees (Gourlet-

Fleury et al., 2023) or site-specific effects (Ligot et al., 2022), could yield a more comprehensive understanding of community-level growth dynamics.

4.2. Seasonal growth patterns: dynamics and variability

The second research question aimed to characterise in detail the seasonal growth patterns observed among the monitored trees and to explore how these patterns differ in their dynamics, as well as to reveal inter- and intraspecific variability. Four distinct growth patterns were identified, ranging from highly seasonal to non-seasonal, with a single tree showing no measurable increment. It is possible that other patterns exist and could be identified with further data collection, particularly given the significant number of individuals excluded from this study. The typology developed here (see section 3.2) could therefore be refined in the future.

Few studies have examined the periodicity of tropical tree growth, and those that have often relied on cambial markers to study ring formation (Angoboy Ilondea et al., 2021; Couralet, 2010; De Mil et al., 2017; Fétéké et al., 2016; Giraldo et al., 2023; Han, 2013; Luse Belanganayi et al., 2024) or, more rarely, on dendrometer measurements (Luse Belanganayi et al., 2024; Plavcová et al., 2025).These studies generally focus on a small number of species and on sites located in different tropical rainforest regions, such as Central Africa (Angoboy Ilondea et al., 2021; Couralet, 2010, 2010; De Mil et al., 2017; Fétéké et al., 2016; Ilondea et al., 2019; Luse Belanganayi et al., 2024), the Amazon (Giraldo et al., 2023), and Asia (Han, 2013). None presents a typology comparable to the one developed here, although some have reported individuals with constant growth (Plavcová et al., 2025) and no-growth (De Mil et al., 2017).

Across these studies, a common conclusion is that water accessibility, particularly the onset and end of the wet periods (precipitation), governs the timing of growth events, and is further supported by the correlation analyses presented in figure 3.10. This observation is consistent with the climatic seasonality of Central Africa, marked by alternating dry and wet periods (Bouvet et al., 2018; F. White, 1983), and could explain the behaviour of the highly and moderately seasonal patterns identified in this work. To confirm these patterns, it will be necessary to continue the planned monitoring to determine whether they are recurrent and to assess whether currently excluded dendrometers display similar or contrasting behaviours. Furthermore, while most cited

studies assume an annual growth rhythm or ring formation, some individuals in the present dataset exhibit cycles of growth and dormancy extending beyond one year. This highlights the importance of extending the dataset before drawing firm conclusions. Installing additional dendrometers on species already identified within each pattern could help confirm these observations or reveal further variability, supporting the broader objectives of the CANOPi project.

A study campaign on wood anatomy along the growth period could be considered to assess whether the seasonal patterns are indeed in phase with the annual formation of growth rings, thereby confirming the existence of the patterns and also helping to understand individuals that have so far produced an unanalysable signal. Figure 4.1 shows a cross-section of two trees for each pattern developed in this work. It can be observed that trees in the seasonal patterns (all deciduous) display well-marked rings, whereas non-seasonal trees (and evergreen) do not present clear ring boundaries. This finding may align with Worbes (1999), who demonstrated in an environment characterised by seasonal rainfall a clear link between precipitation patterns and the formation of tree rings.

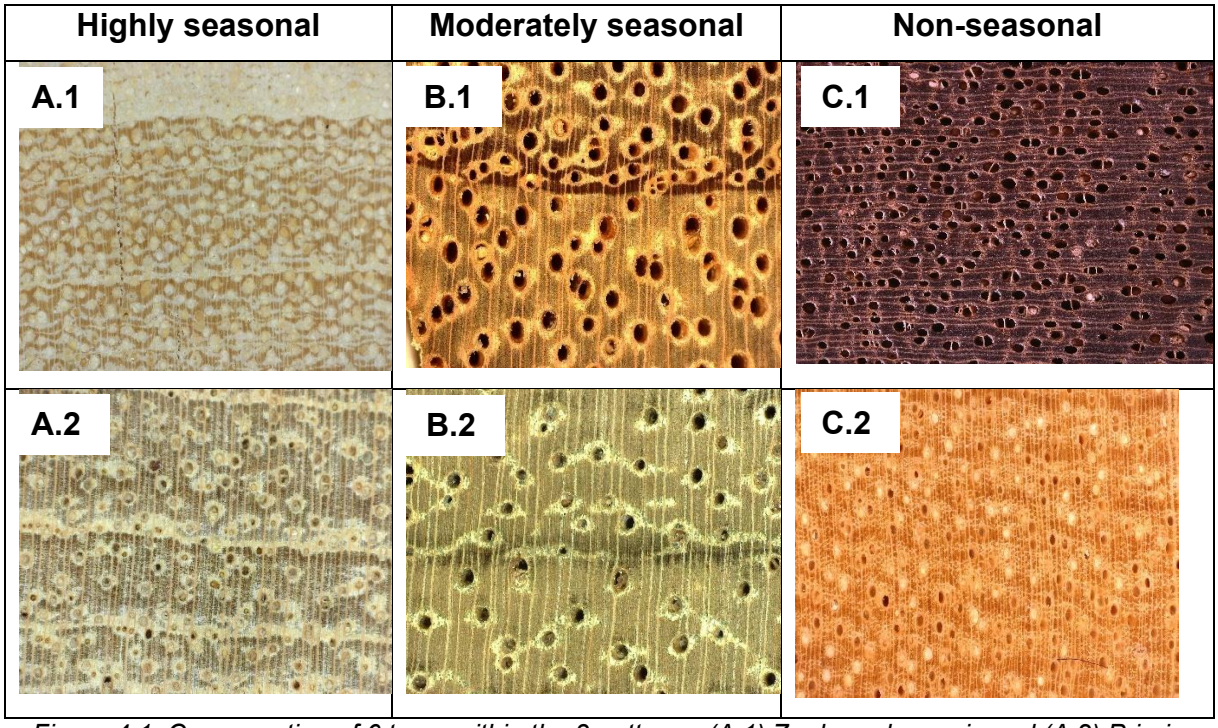

Figure 4.1: Cross section of 6 trees within the 3 patterns: (A.1) Zanha golugensis and (A.2) Prioria balsamifera as highly seasonal, (B.1) Piptadenisatrum africanum and (B.2) Miliciea excelsa as moderately seasonal, (C.1) Guarea cedrata and (C.2) Ongokea gore. Picture come from InsideWood data base.

Among the trees classified as seasonal, based on growth curves showing alternating phases of growth and stagnation, the majority are deciduous. This finding reinforces the explanation of overall community seasonality presented in the previous section, as these alternations may be closely linked to leaf phenology (Angoboy Ilondea et al., 2021). Another notable feature of seasonal patterns is the variability in growth onset and cessation: while growth initiation is highly variable among individuals, cessation is much more synchronised. Given the dominance of deciduous trees in these patterns, this behaviour appears linked both to growth dynamics and to the onset of the rainy season. It is already clear that growth occurs during the rainy season, from October to May. However, breakpoint analysis reveals substantial variability in growth onset dates. Historical phenological studies at Luki show that defoliation occurs at the end of the dry season, quickly followed by leaf flushing (Angoboy Ilondea et al., 2021; Couralet et al., 2013), but these events are not synchronous across trees, with peak defoliation between September and October (Couralet et al., 2013). Given the potential close link between leaf flushing and radial growth, these results suggest that the onset of radial growth is strongly associated with leaf emergence, explaining the observed variability. By contrast, the end of growth appears more synchronised with the start of the dry season, even though defoliation only occurs at its end. The comparison between the patterns observed in this study and data extracted from phenocams, which continuously capture images of the crowns of the trees studied here, will make it possible to confirm or refute the considerations presented above.

Couralet et al. (2013) also document the presence of trees more accurately described as “leaf exchangers,” a functional type defined by Singh and Kushwaha (2005), rather than strictly deciduous. In such trees, leaf flushing occurs immediately after or even during leaf loss, maintaining continuous canopy cover. These trees are also referred as brevi-deciduous. This may explain why moderately seasonal trees still show measurable radial growth during stagnation phases. The presence of evergreen trees among the non-seasonal group supports the link between canopy persistence and continuous radial growth. The remaining non-seasonal trees may also be “leaf exchangers” with a high turnover rate, functionally resembling evergreens. Integrating phenocam observations could provide valuable confirmation of these interpretations.

The pattern descriptions also reveal substantial interspecific variability, visible in their classification as well as in the duration, onset, cessation, and intensity of growth

periods. This variability is also expressed within species. For instance, *Piptadeniastrum africanum* (deciduous) appears in both the moderately seasonal and non-seasonal categories, suggesting that it may actually behave as a “leaf exchanger.” It is also important to acknowledge the trees that were excluded from the analysis for reasons previously discussed. They likely represent a substantial portion of inter- and intraspecific variability that cannot currently be quantified. Additional data will be required to better understand their growth behaviour. In addition, some trees equipped with two dendrometers displayed differing growth curves within the same pattern, indicating asymmetrical radial growth. Such asymmetries may result from micro-environmental influences, such as wind, slope, competition, exposure, or local moisture conditions (H. Wang et al., 2023). These findings highlight both a limitation of point-based dendrometer measurements and the importance of considering fine-scale environmental variability. A targeted campaign to monitor micro-environmental parameters could therefore help explain these growth differences. For example, “leaf exchangers” experiencing high soil moisture levels might functionally behave like evergreens (Singh & Kushwaha, 2005).

4.3. Climatic and environmental influence

The third research question aimed to assess the extent to which the identified growth patterns are influenced by climatic conditions. The most striking result is the direct link between the growth periods of seasonal patterns and the rainy season, which confirms the conclusions previously discussed (figure 3.9).

During the growth period, vapour pressure deficit (VPD), temperature, and solar radiation tend to increase, which aligns with findings from previous studies conducted at Luki (De Mil et al., 2019). In addition, a certain level of soil water content appears to be required for growth to begin, while a decline in soil moisture helps explain the end of the growth period. When the volume of extractable water becomes sufficient or insufficient, it has direct implications for radial growth (Kühnhammer et al., 2023; Meir et al., 2015). Trees with deeper root systems may therefore show greater radial growth and likely greater resilience to drought episodes (Kühnhammer et al., 2023).

The correlation plots between climatic variables confirm a notable relationship between precipitation and soil water content (figure 3.10), both at the onset and at the end of

growth periods. This is supported by the conclusions of Plavcová et al. (2025), who conducted a similar analysis. These findings confirm that seasonality in Central Africa is clearly governed by the alternation between dry and wet seasons. However, field-based measurements of soil water content are needed, given the limitations of ERA5 data in this regard (Muñoz-Sabater et al., 2021; Yang et al., 2022). In the context of climate change, future projections indicating more intense dry periods are therefore likely to have a direct impact on the dynamics of Central African forest ecosystems.

4.4. Additional insights from Gompertz growth modelling

While the previous section focused on identifying the timing of growth phases in relation to climatic variables, the Gompertz growth model provided an additional quantitative perspective. This approach allowed the extraction of precise parameters for each growth phase, including the maximum growth rate, the timing of the inflection point, and the duration of active growth. Such metrics offer valuable insight into inter- and intraspecific variability.

Importantly, the detection of growth onset and cessation also confirmed the robustness of the breakpoint analysis. While the Gompertz model indicated that the main growth phase occurred between mid-December and mid-June (figure 3.11), the breakpoint analysis for the highly seasonal pattern detected growth onset between late October and early February, with growth cessation between March and June (most frequently around June) (see section 9.3a). The general agreement between these two approaches supports the reliability of the breakpoint method for capturing the main phases of radial growth.

The inflection point, corresponding to the period of highest growth rate, most often occurs between January and February. This timing follows the month with the highest rainfall and coincides with the transition towards the lowest monthly rainfall within the rainy season, which may correspond to the short dry season observed at Luki (Couralet et al., 2013). This pattern supports the conclusion that growth is sustained by water availability. Despite the variability in the onset of growth among different trees, the start of growth slowdown tends to occur at roughly the same time each year. This suggests that the beginning of the deceleration phase is not influenced by the onset of the growth period. Although growth continues after the inflection point, the end of growth is less

variable and most often coincides with the end of the rainy season. Looking ahead, if climate change results in longer and more intense dry seasons in Central Africa, growth is likely to be less sustained. A reduction in rainfall could cause the inflection point to occur earlier and the onset of the dry season to advance, thereby shortening the total growth period. This will also have implications for carbon dynamics, given the role that trees, and especially tropical forests, play in this process (Rachel, 2014).

Gompertz modelling would therefore be valuable to repeat in the coming years, ideally with a larger number of individuals to improve the fit of the models. This would make it possible to assess whether the parameters derived from the model change over time and how they are affected by concurrent climatic measurements.

5. Conclusion

This study provides new insights into the intra- and interspecific variability of radial growth patterns in a Central African tropical forest, based on high-resolution dendrometer measurements. By classifying individuals into four distinct patterns, ranging from highly seasonal to non-seasonal, it was possible to identify key differences in growth timing, duration, and intensity and to link these differences environmental conditions. The growth dynamics are largely governed by seasonality, with the majority of growth taking place during the wet season. This underscores the pivotal role of water availability in regulating tree growth in Central Africa.

The analysis also highlights the importance of considering both species-level traits, such as leaf habit, and micro-environmental factors, which can influence growth behaviour even within the same species. Limitations remain, notably the exclusion of a significant proportion of dendrometers, the relatively short observation period, and the absence of direct micro-environmental and phenological data.

Future work should focus on extending the monitoring period, increasing the number of instrumented individuals, and integrating complementary approaches, such as microclimate measurements, dendroanatomy studies and modelling approaches like the Gompertz function. The integration of other data from the CANOPi experimental set-up will also provide valuable insights into the functioning of Central African ecosystems, by linking tree-level processes to broader ecological and climatic dynamics. The methodology developed in this study can be deployed across the different CANOPi monitoring sites, enabling comparative analyses between regions and improving our understanding of spatial variability in growth responses. Such efforts would allow for a more robust characterisation of growth patterns, a better understanding of their drivers, and improved capacity to detect long-term shifts under climate change.

Beyond the scope of this study, these findings have broader implications for understanding carbon dynamics in tropical forests. As these ecosystems play a pivotal role in the global carbon cycle, any change in the timing or magnitude of wood growth, particularly under scenarios of altered rainfall regimes, could significantly impact carbon storage and ecosystem functioning.

6. Personal contribution

First, during my internship at the Luki Biosphere Reserve, I was able to familiarise myself with all the experimental setups of the CANOPi project, including the dendrometers. I took part in the maintenance and data collection in the field for the dendrometers. This thesis therefore follows on logically from that experience.

To meet the objectives of this thesis, I established a solid foundation for the full analysis of the dendrometers installed under the CANOPi project using RStudio. This required becoming familiar with a very large dataset, understanding it, cleaning it, and preparing it while keeping the objectives of this work in mind. It then involved developing appropriate methods to obtain results consistent with these objectives. The process developed here can now be applied to other dendrometers within the CANOPi project and beyond.

Finally, I would like to note in this section that AI (in this case ChatGPT) was used as support for solving coding issues, as a translation tool, and as an aid for spelling and grammar in English.

7. References

Angoboy Ilondea, B., Beeckman, H., Van Acker, J., Van den Bulcke, J., Fayolle, A., Couralet, C., Hubau, W., Kafuti, C., Rousseau, M., Kaka di-Makwala, A., Bourland, N., Deklerck, V., Kasongo Yakusu, E., Ewango, C., & De Mil, T. (2021). Variation in Onset of Leaf Unfolding and Wood Formation in a Central African Tropical Tree Species. *Frontiers in Forests and Global Change*, *4*. https://doi.org/10.3389/ffgc.2021.673575

Artaxo, P., Hansson, H. C., Machado, L. A. T., & Rizzo, L. V. (2022). Tropical forests are crucial in regulating the climate on Earth. *PLOS Climate*, *1*(8), e0000054. https://doi.org/10.1371/journal.pclm.0000054

Bai, J., & Perron, P. (2003). Computation and analysis of multiple structural change models. *Journal of Applied Econometrics*, *18*(1), 1-22. https://doi.org/10.1002/jae.659

Beck, H. E., Zimmermann, N. E., McVicar, T. R., Vergopolan, N., Berg, A., & Wood, E. F. (2018). Present and future Köppen-Geiger climate classification maps at 1-km resolution. *Scientific Data*, *5*(1), 180214. https://doi.org/10.1038/sdata.2018.214

Bennett, A. C., Dargie, G. C., Cuni-Sanchez, A., Tshibamba Mukendi, J., Hubau, W., Mukinzi, J. M., Phillips, O. L., Malhi, Y., Sullivan, M. J. P., Cooper, D. L. M., Adu-Bredu, S., Affum-Baffoe, K., Amani, C. A., Banin, L. F., Beeckman, H., Begne, S. K., Bocko, Y. E., Boeckx, P., Bogaert, J., … Lewis, S. L. (2021). Resistance of African tropical forests to an extreme climate anomaly. *Proceedings of the National Academy of Sciences*, *118*(21). https://doi.org/10.1073/pnas.2003169118

Bienu, S., Lubalega, T., Khasa, D., David, K. K., Yang, L., Yuhua, L., Eyul'Anki, D., Tango, E., & Katula, H. (2023). Floristic Diversity and structural parameters on the forest tree population in the Luki Biosphere Reserve, Democratic Republic of Congo. *Global Ecology and Conservation*, *44*, e02489. https://doi.org/10.1016/j.gecco.2023.e02489

Bouvet, A., Mermoz, S., Le Toan, T., Villard, L., Mathieu, R., Naidoo, L., & Asner, G. (2018). An above-ground biomass map of African savannahs and woodlands at 25 m resolution derived from ALOS PALSAR. *Remote Sensing of Environment*, *206*, 156-173. https://doi.org/10.1016/j.rse.2017.12.030

Bush, E. R., Jeffery, K., Bunnefeld, N., Tutin, C., Musgrave, R., Moussavou, G., Mihindou, V., Malhi, Y., Lehmann, D., Ndong, J. E., Makaga, L., & Abernethy, K. (2020).

Rare ground data confirm significant warming and drying in western equatorial Africa. *PeerJ*, *8*, e8732. https://doi.org/10.7717/peerj.8732

Bush, E. R., Jeffery, K., Bunnefeld, N., Tutin, C., Musgrave, R., Moussavou, G., Mihindou, V., Malhi, Y., Lehmann, D., Ndong, J. E., Makaga, L., & Abernethy, K. A. (2019). *Ground data confirm warming and drying are at a critical level for forest survival in western equatorial Africa* (No. e27848v1). PeerJ Inc. https://doi.org/10.7287/peerj.preprints.27848v1

Cavaleri, M. A., Reed, S. C., Smith, W. K., & Wood, T. E. (2015). Urgent need for warming experiments in tropical forests. *Global Change Biology*, *21*(6), 2111-2121. https://doi.org/10.1111/gcb.12860

Chen, K., Cai, Q., Zheng, N., Li, Y., Lin, C., & Li, Y. (2021). Forest Carbon Sink Evaluation – An Important Contribution for Carbon Neutrality. *IOP Conference Series: Earth and Environmental Science*, *811*(1), 012009. https://doi.org/10.1088/1755-1315/811/1/012009

Cleveland, W. S., & Devlin, S. J. (1988). *Locally Weighted Regression:An Approach to Regression Analysis by Local Fitting*.

Couralet, C. (2010). *Community dynamics, phenology and growth of tropical trees in the rain forest reserve of Luki, Democratic Republic of Congo* [Dissertation, Ghent University]. http://hdl.handle.net/1854/LU-1028918

Couralet, C., Van den Bulcke, J., Ngoma, L. M., Van Acker, J., & Beeckman, H. (2013). Phenology in functional groups of Central African rainforest trees. *JOURNAL OF TROPICAL FOREST SCIENCE*, *25*(3), Article 3.

Cuny, H., Rathgeber, C., Frank, D., Fonti, P., Mäkinen, H., Prislan, P., Rossi, S., Martinez del Castillo, E., Campelo, F., Vavrčík, H., Camarero, J., Bryukhanova, M., Jyske, T., Gricar, J., Gryc, V., de Luis, M., Vieira, J., Cufar, K., Kirdyanov, A., & Fournier, M. (2015). Woody biomass production lags stem-girth increase by over one month in coniferous forests. *Nature Plants*, *Article number: 15160*, 1-6. https://doi.org/10.1038/NPLANTS.2015.160

Cusack, D., Reed, S., Andersen, K., Cinoğlu, D., Craig, M., Dietterich, L., Hogan, J. A., Holm, J., Nottingham, A., Ostertag, R., Soper, F., Wood, T., & Wong, M. (2024). Tropical forests and global change : Biogeochemical responses and opportunities for cross-site

comparisons, an organized INSPIRE session at the 108 Annual Meeting, Ecological Society of America, Portland, Oregon, USA, August 2023. *New Phytologist*, *241*. https://doi.org/10.1111/nph.19511

De Mil, T., Hubau, W., Angoboy Ilondea, B., Rocha Vargas, M. A., Boeckx, P., Steppe, K., Van Acker, J., Beeckman, H., & Van den Bulcke, J. (2019). Asynchronous leaf and cambial phenology in a tree species of the Congo Basin requires space–time conversion of wood traits. *Annals of Botany*, *124*(2), 245-253. https://doi.org/10.1093/aob/mcz069

De Mil, T., Ilondea Bhely, A., Maginet, S., Duvillier, J., Van Acker, J., Beeckman, H., & Van den Bulcke, J. (2017). Cambial activity in the understory of the Mayombe forest, DR Congo. *Trees*, *31*. https://doi.org/10.1007/s00468-016-1454-x

De Swaef, T., De Schepper, V., Vandegehuchte, M. W., & Steppe, K. (2015). Stem diameter variations as a versatile research tool in ecophysiology. *Tree Physiology*, *35*(10), 1047-1061. https://doi.org/10.1093/treephys/tpv080

Diedhiou, A., Bichet, A., Wartenburger, R., Seneviratne, S. I., Rowell, D. P., Sylla, M. B., Diallo, I., Todzo, S., Touré, N. E., Camara, M., Ngatchah, B. N., Kane, N. A., Tall, L., & Affholder, F. (2018). Changes in climate extremes over West and Central Africa at 1.5 °C and 2 °C global warming. *Environmental Research Letters*, *13*(6), 065020. https://doi.org/10.1088/1748-9326/aac3e5

Digital Earth Africa. (2025). *Digital Earth Africa*. retrieved June 17, 2025, sur https://digitalearthafrica.org/en_za/

Djomo, A. N., Picard, N., Fayolle, A., Henry, M., Ngomanda, A., Ploton, P., McLellan, J., Saborowski, J., Adamou, I., & Lejeune, P. (2016). Tree allometry for estimation of carbon stocks in African tropical forests. *Forestry: An International Journal of Forest Research*, *89*(4), 446-455. https://doi.org/10.1093/forestry/cpw025

Fan, Z.-X., Bräuning, A., Fu, P.-L., Yang, R.-Q., Qi, J.-H., Grießinger, J., & Gebrekirstos, A. (2019). Intra-Annual Radial Growth of Pinus kesiya var. Langbianensis Is Mainly Controlled by Moisture Availability in the Ailao Mountains, Southwestern China. *Forests*, *10*(10), Article 10. https://doi.org/10.3390/f10100899

Fayaz, A., Chaudhary, P., & Mankotia, S. (2025). Impacts of Climate Change on Forest Ecosystem Dynamics and Management Strategies. *International Journal of Environment and Climate Change*, *15*(1), 273-286. https://doi.org/10.9734/ijecc/2025/v15i14691

Fétéké, F., Fayolle, A., Dainou, K., Bourland, N., Dié, A., Lejeune, P., Doucet, J.-L., & Beeckman, H. (2016). VARIATIONS SAISONNIÈRES DE LA CROISSANCE DIAMÉTRIQUE ET DES PHÉNOLOGIES FOLIAIRE ET REPRODUCTIVE DE TROIS ESPÈCES LIGNEUSES COMMERCIALES D'AFRIQUE CENTRALE. *BOIS & FORETS DES TROPIQUES*, *330*, 3-21. https://doi.org/10.19182/bft2016.330.a31315

Fotso-Nguemo, T. C., Diallo, I., Diakhaté, M., Vondou, D. A., Mbaye, M. L., Haensler, A., Gaye, A. T., & Tchawoua, C. (2019). Projected changes in the seasonal cycle of extreme rainfall events from CORDEX simulations over Central Africa. *Climatic Change*, *155*(3), 339-357. https://doi.org/10.1007/s10584-019-02492-9

Giraldo, J. A., del Valle, J. I., González-Caro, S., David, D. A., Taylor, T., Tobón, C., & Sierra, C. A. (2023). Tree growth periodicity in the ever-wet tropical forest of the Americas. *Journal of Ecology*, *111*(4), 889-902. https://doi.org/10.1111/1365-2745.14069

Gorel, A.-P. (2025). *Leaf habit, maximum height, and wood density of tropical woody flora in Africa : Phylogenetic constraints, covariation, and responses to seasonal drought* (Version 4, p. 232567 bytes) [data set]. Dryad. https://doi.org/10.5061/DRYAD.Q573N5TTN

Gourlet-Fleury, S., Rossi, V., Forni, E., Fayolle, A., Ligot, G., Allah-Barem, F., Baya, F., Bénédet, F., Boyemba, F., Cornu, G., Doucet, J.-L., Gillet, J.-F., Mazengue, M., Mbasi Mbula, M., Van Hoef, Y., Zombo, I., & Freycon, V. (2023). Competition and site weakly explain tree growth variability in undisturbed Central African moist forests. *Journal of Ecology*, *111*(9), 1950-1967. https://doi.org/10.1111/1365-2745.14152

Guan, K., Pan, M., Li, H., Wolf, A., Wu, J., Medvigy, D., Caylor, K. K., Sheffield, J., Wood, E. F., Malhi, Y., Liang, M., Kimball, J. S., Saleska, S. R., Berry, J., Joiner, J., & Lyapustin, A. I. (2015). Photosynthetic seasonality of global tropical forests constrained by hydroclimate. *Nature Geoscience*, *8*(4), 284-289. https://doi.org/10.1038/ngeo2382

Han, K. (2013). *The Dynamics of Radial Growth of Three Selected Tropical Tree Species Studied through Knife-cutting Method*.

Harrison, I., Brummett, R., & Stiassny, M. (2016). *Congo River Basin* (p. 1-18). https://doi.org/10.1007/978-94-007-6173-5_92-2

Hubau, W., Lewis, S., Phillips, O., Affum-Baffoe, K., Beeckman, H., cuni sanchez, A., Daniels, A., Ewango, C., Fauset, S., Mukinzi, J., Sheil, D., Sonké, B., Sullivan, M., Sunderland, T., Taedoumg, H., Thomas, S., White, L., Abernethy, K., Adu-Bredu, S., & Zemagho, L. (2020). Asynchronous Carbon Sink Saturation in African and Amazonian Tropical Forests. *Nature*, *579*.

Hui, D., Deng, Q., Tian, H., & Luo, Y. (2017). Climate Change and Carbon Sequestration in Forest Ecosystems. In *Handbook of Climate Change Mitigation and Adaptation* (p. 555-594). Springer, Cham. https://doi.org/10.1007/978-3-319-14409-2_13

Ilondea, B. A., Beeckman, H., Ouedraogo, D.-Y. O., Bourland, N., Mil, T. D., Bulcke, J. V. D., Acker, J. V., Couralet, C., Ewango, C., Hubau, W., Toirambe, B., Doucet, J.-L., & Fayolle, A. (2019). Une forte saisonnalité du climat et de la phénologie reproductive dans la forêt du Mayombe : L'apport des données historiques de la Réserve de Luki en République démocratique du Congo. *BOIS & FORETS DES TROPIQUES*, *341*, 39-53. https://doi.org/10.19182/bft2019.341.a31753

InsideWood. 2004-onwards. Published on the Internet. http://insidewood.lib.ncsu.edu/search [08-13-2025].

Kaewmano, A., Fu, P.-L., Fan, Z.-X., Pumijumnong, N., Zuidema, P. A., & Bräuning, A. (2022). Climatic influences on intra-annual stem radial variations and xylem formation of *Toona ciliata* at two Asian tropical forest sites with contrasting soil water availability. *Agricultural and Forest Meteorology*, *318*, 108906. https://doi.org/10.1016/j.agrformet.2022.108906

Kasongo Yakusu, E., Van Acker, J., Van De Vyver, H., Bourland, N., Mbifo Ndiapo, J., Besango Likwela, T., Lokonda Wa Kipifo, M., Mbuya Kankolongo, A., Van Den Bulcke, J., Beeckman, H., Bauters, M., Boeckx, P., Verbeeck, H., Jacobsen, K., Demarée, G., Gellens-Meulenberghs, F., & Hubau, W. (2023). Ground-based climate data show evidence of warming and intensification of the seasonal rainfall cycle during the 1960–

2020 period in Yangambi, central Congo Basin. *Climatic Change*, *176*(10). https://doi.org/10.1007/s10584-023-03606-0

Kruskal, W. H., & Wallis, W. A. (1952). Use of Ranks in One-Criterion Variance Analysis. *Journal of the American Statistical Association*, *47*(260), 583-621. https://doi.org/10.1080/01621459.1952.10483441

Kühnhammer, K., van Haren, J., Kübert, A., Bailey, K., Dubbert, M., Hu, J., Ladd, S. N., Meredith, L. K., Werner, C., & Beyer, M. (2023). Deep roots mitigate drought impacts on tropical trees despite limited quantitative contribution to transpiration. *The Science of the Total Environment*, *893*, 164763. https://doi.org/10.1016/j.scitotenv.2023.164763

Kümmel, A., Bonate, P. L., Dingemanse, J., & Krause, A. (2018). Confidence and Prediction Intervals for Pharmacometric Models. *CPT: Pharmacometrics & Systems Pharmacology*, *7*(6), 360-373. https://doi.org/10.1002/psp4.12286

Lewis, S., Lopez-Gonzalez, G., Sonké, B., Affum-Baffoe, K., Baker, T., Ojo, L., Phillips, O., Reitsma, J., White, L., Comiskey, J., Djuikouo, M., Ewango, C., Feldpausch, T., Hamilton, A., Gloor, M., Hart, T., Hladik, A., Lloyd, J., Lovett, J., & Wöll, H. (2009). Increasing Carbon Storage in Intact African Tropical Forests. *Nature*, *457*, 1003-1006. https://doi.org/10.1038/nature07771

Ligot, G., Gourlet-Fleury, S., Dainou, K., Gillet, J.-F., Rossi, V., Mazengué, M., Ekome, S. N., Nkoulou, Y. S., Zombo, I., Forni, E., & Doucet, J.-L. (2022). Tree growth and mortality of 42 timber species in central Africa. *Forest Ecology and Management*, *505*, 119889. https://doi.org/10.1016/j.foreco.2021.119889

Lindquist, E. J., Food and Agriculture Organization of the United Nations, & European Commission (Éds.). (2012). *Global forest land-use change, 1990-2005*. Food and Agriculture Organization of the United Nations.

Lubini, A. (1997). *La végétation de la Réserve de biosphère de Luki au Mayombe (Zaïre)*. Jardin botanique national de Belgique.

Luse Belanganayi, B., Ilondea, B. A., Phaka, C. M., Laurent, F., Djiofack, B. Y., Kafuti, C., Peters, R. L., Bourland, N., Beeckman, H., & De Mil, T. (2024). Diel and annual rhythms of tropical stem size changes in the Mayombe forest, Congo Basin. *Frontiers in Forests and Global Change*, *7*. https://doi.org/10.3389/ffgc.2024.1185225

Mayaux, P., Pekel, J.-F., Desclée, B., Donnay, F., Lupi, A., Frédéric, A., Clerici, M., Bodart, C., Brink, A., Nasi, R., & Belward, A. (2013). State and evolution of the African rainforests between 1990 and 2010. *Philosophical transactions of the Royal Society of London. Series B, Biological sciences*, *368*, 20120300. https://doi.org/10.1098/rstb.2012.0300

Meir, P., Wood, T. E., Galbraith, D. R., Brando, P. M., Da Costa, A. C. L., Rowland, L., & Ferreira, L. V. (2015). Threshold Responses to Soil Moisture Deficit by Trees and Soil in Tropical Rain Forests : Insights from Field Experiments. *BioScience*, *65*(9), 882-892. https://doi.org/10.1093/biosci/biv107

Muñoz-Sabater, J., Dutra, E., Agustí-Panareda, A., Albergel, C., Arduini, G., Balsamo, G., Boussetta, S., Choulga, M., Harrigan, S., Hersbach, H., Martens, B., Miralles, D. G., Piles, M., Rodríguez-Fernández, N. J., Zsoter, E., Buontempo, C., & Thépaut, J.-N. (2021). ERA5-Land : A state-of-the-art global reanalysis dataset for land applications. *Earth System Science Data*, *13*(9), 4349-4383. https://doi.org/10.5194/essd-13-4349-2021

Opelele Omeno, M., Yu, Y., Fan, W., Lubalega, T., Chen, C., & Kachaka Sudi Kaiko, C. (2021). Analysis of the Impact of Land-Use/Land-Cover Change on Land-Surface Temperature in the Villages within the Luki Biosphere Reserve. *Sustainability*, *13*(20), Article 20. https://doi.org/10.3390/su132011242

Peel, M., Finlayson, B., & Mcmahon, T. (2007). Updated World Map of the Koppen-Geiger Climate Classification. *Hydrology and Earth System Sciences Discussions*, *4*. https://doi.org/10.5194/hess-11-1633-2007

Pinheiro, J., Bates, D., & R Core Team. (1999). *nlme : Linear and Nonlinear Mixed Effects Models* (p. 3.1-168). https://doi.org/10.32614/CRAN.package.nlme

Plavcová, L., Tumajer, J., Altman, J., Svoboda, M., Stegehuis, A. I., Pejcha, V., & Doležal, J. (2025). High Inter-Specific Diversity and Seasonality of Trunk Radial Growth in Trees Along an Afrotropical Elevational Gradient. *Plant, Cell & Environment*, *48*(3), 2285-2297. https://doi.org/10.1111/pce.15295

Prediction of Worldwide Energy Resources (POWER) Project. (2025). Data obtained from the National Aeronautics and Space Administration (NASA) Langley Research

Center's POWER Project. Retrieved June 17, 2025, from https://registry.opendata.aws/nasa-power

Rachel, G. (2014). Ecology of Tropical Rain Forests. In *Ecology and the Environment* (p. 247-272). https://doi.org/10.1007/978-1-4614-7501-9_4

Román-Palacios, C., & Wiens, J. J. (2020). Recent responses to climate change reveal the drivers of species extinction and survival. *Proceedings of the National Academy of Sciences*, *117*(8), 4211-4217. https://doi.org/10.1073/pnas.1913007117

Root, T., Price, J., Hall, K., Schneider, S., Rosenzweig, C., & Pounds, A. (2003). Fingerprints of global warming on wild animals and plants. *Nature*, *421*, 57-60. https://doi.org/10.1038/nature01333

Sénéchal, J., Kabala, D. M., & Fournier, F. (1989). *Revue des connaissances sur le Mayombe—UNESCO Digital library* https://unesdoc.unesco.org/ark:/48223/pf0000086519

Silva de Miranda, P. L., Dexter, K. G., Swaine, M. D., de Oliveira-Filho, A. T., Hardy, O. J., & Fayolle, A. (2022). Dissecting the difference in tree species richness between Africa and South America. *Proceedings of the National Academy of Sciences*, *119*(14), e2112336119. https://doi.org/10.1073/pnas.2112336119

Silvestro, R., Deslauriers, A., Prislan, P., Rademacher, T., Rezaie, N., Richardson, A. D., Vitasse, Y., & Rossi, S. (2025). From Roots to Leaves : Tree Growth Phenology in Forest Ecosystems. *Current Forestry Reports*, *11*(1), 12. https://doi.org/10.1007/s40725-025-00245-9

Singh, K., & Kushwaha, C. (2005). Emerging paradigms of tree phenology in dry tropics. *Current Science*, *89*.

Sullivan, M. J. P., Lewis, S. L., Affum-Baffoe, K., Castilho, C., Costa, F., Sanchez, A. C., Ewango, C. E. N., Hubau, W., Marimon, B., Monteagudo-Mendoza, A., Qie, L., Sonké, B., Martinez, R. V., Baker, T. R., Brienen, R. J. W., Feldpausch, T. R., Galbraith, D., Gloor, M., Malhi, Y., … Phillips, O. L. (2020). Long-term thermal sensitivity of Earth's tropical forests. *Science*, *368*(6493), 869-874. https://doi.org/10.1126/science.aaw7578

Thomas, C. D., Cameron, A., Green, R. E., Bakkenes, M., Beaumont, L. J., Collingham, Y. C., Erasmus, B. F. N., de Siqueira, M. F., Grainger, A., Hannah, L., Hughes, L., Huntley, B., van Jaarsveld, A. S., Midgley, G. F., Miles, L., Ortega-Huerta, M. A., Townsend Peterson, A., Phillips, O. L., & Williams, S. E. (2004). Extinction risk from climate change. *Nature*, *427*(6970), 145-148. https://doi.org/10.1038/nature02121

Tiersmondo Longandjo, G.-N., & Rouault, M. (2023). *Revisiting the Seasonal Cycle of Rainfall over Central Africa*. https://doi.org/10.21203/rs.3.rs-2956778/v1

Uddin, M. F., & Chaudhry, A. G. (2024). Assessing the Impact of Climate Change on Global Biodiversity : Trends and Predictions. *International Journal of Trends and Innovations in Business & Social Sciences*, *2*(2), Article 2. https://doi.org/10.48112/tibss.v2i2.803

Vanoni, M., Bugmann, H., Nötzli, M., & Bigler, C. (2016). Quantifying the effects of drought on abrupt growth decreases of major tree species in Switzerland. *Ecology and Evolution*, *6*(11), 3555-3570. https://doi.org/10.1002/ece3.2146

Vieilledent, G., Fischer, F. J., Chave, J., Guibal, D., Langbour, P., & Gérard, J. (2023). *Code and data for : New formula and conversion factor to compute basic wood density of tree species using a global wood technology database.* (Version 2) [data set]. CIRAD Dataverse. https://doi.org/10.18167/DVN1/KRVF0E

Wagner, F., Rossi, V., Aubry-Kientz, M., Bonal, D., Dalitz, H., Gliniars, R., Stahl, C., Trabucco, A., & Hérault, B. (2014). Pan-Tropical Analysis of Climate Effects on Seasonal Tree Growth. *PLOS ONE*, *9*(3), e92337. https://doi.org/10.1371/journal.pone.0092337

Wang, H., Qin, J., Hu, Y., & Guo, C. (2023). Asymmetric growth of belowground and aboveground tree organs and their architectural relationships : A review. *Canadian Journal of Forest Research*, *53*(5), 315-327. https://doi.org/10.1139/cjfr-2022-0216

Wang, J., Li, W., Ciais, P., Ballantyne, A., Goll, D., Huang, X., Zhao, Z., & Zhu, L. (2020). Changes in Biomass Turnover Times in Tropical Forests and Their Environmental Drivers From 2001 to 2012. *Earth's Future*, *9*. https://doi.org/10.1029/2020EF001655

White, F. (1983). *The Vegetation of Africa; a descriptive memoir to accompany the UNESCO/AETFAT/UNSO vegetation map of Africa—UNESCO Digital Library*. https://unesdoc.unesco.org/ark:/48223/pf0000058054

White, L. J. T., Masudi, E. B., Ndongo, J. D., Matondo, R., Soudan-Nonault, A., Ngomanda, A., Averti, I. S., Ewango, C. E. N., Sonké, B., & Lewis, S. L. (2021). Congo Basin rainforest—Invest US$150 million in science. *Nature*, *598*(7881), 411-414. https://doi.org/10.1038/d41586-021-02818-7

Wilcoxon, F. (1945). Individual Comparisons by Ranking Methods. *Biometrics Bulletin*, *1*(6), 80-83. https://doi.org/10.2307/3001968

Worbes, M. (1999). Annual growth rings, rainfall-dependent growth and long-term growth patterns of tropical trees from the Caparo Forest Reserve in Venezuela. *Journal of Ecology*, *87*(3), 391-403. https://doi.org/10.1046/j.1365-2745.1999.00361.x

Yaduv, V. K., Srivastava, A. K., & Khare, P. K. (2018). Tropical Forest and Ecosystem Services in Indian Context. *Current World Environment*, *13*(1), 151-158. https://doi.org/10.12944/CWE.13.1.14

Yang, S., Zeng, J., Fan, W., & Cui, Y. (2022). Evaluating Root-Zone Soil Moisture Products from GLEAM, GLDAS, and ERA5 Based on In Situ Observations and Triple Collocation Method over the Tibetan Plateau. *Journal of Hydrometeorology*, *23*(12), 1861-1878. https://doi.org/10.1175/JHM-D-22-0016.1

Zanne, A., Lopez-Gonzalez, G., Coomes, D., & David, A. (2009). *Data from : Towards a worldwide wood economics spectrum [Dataset]. Dryad.* https://doi.org/10.5061/dryad.234

Zeide, B. (1993). Analysis of Growth Equations. *Forest Science*, *39*(3), 594-616. https://doi.org/10.1093/forestscience/39.3.594

Zeileis, A., Leisch, F., Hornik, K., & Kleiber, C. (2002). Strucchange : An R Package for Testing for Structural Change in Linear Regression Models. *Journal of Statistical Software*, *7*, 1-38. https://doi.org/10.18637/jss.v007.i02

Zhou, B., Sterck, F., Kruijt, B., Fan, Z.-X., & Zuidema, P. A. (2023). Diel and seasonal stem growth responses to climatic variation are consistent across species in a

subtropical tree community. *New Phytologist*, *240*(6), 2253-2264. https://doi.org/10.1111/nph.19275

Zweifel, R. (2015). Radial stem variations : A source of tree physiological information not fully exploited yet. *Plant, cell & environment*, *39*. https://doi.org/10.1111/pce.12613

8. Appendix

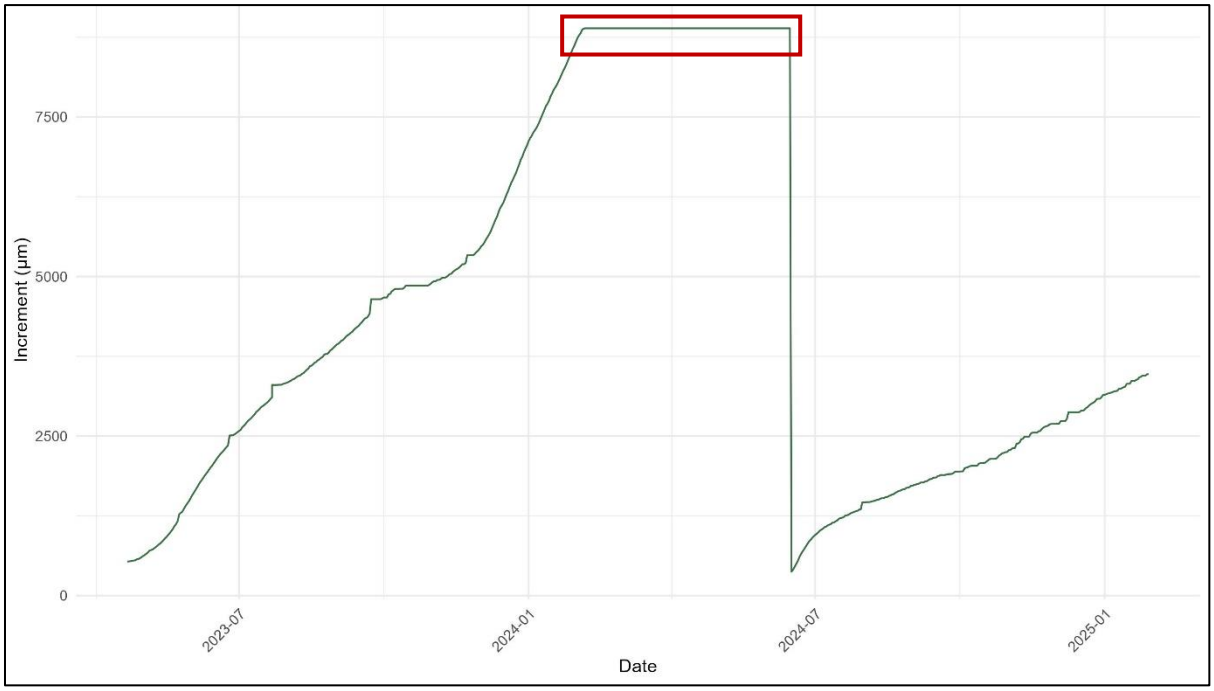

Figure A1: Increment curves recorded by a dendrometer (92232083 – Desbordesia glaucescens), which shows saturation highlighted in red and is therefore excluded from the study.

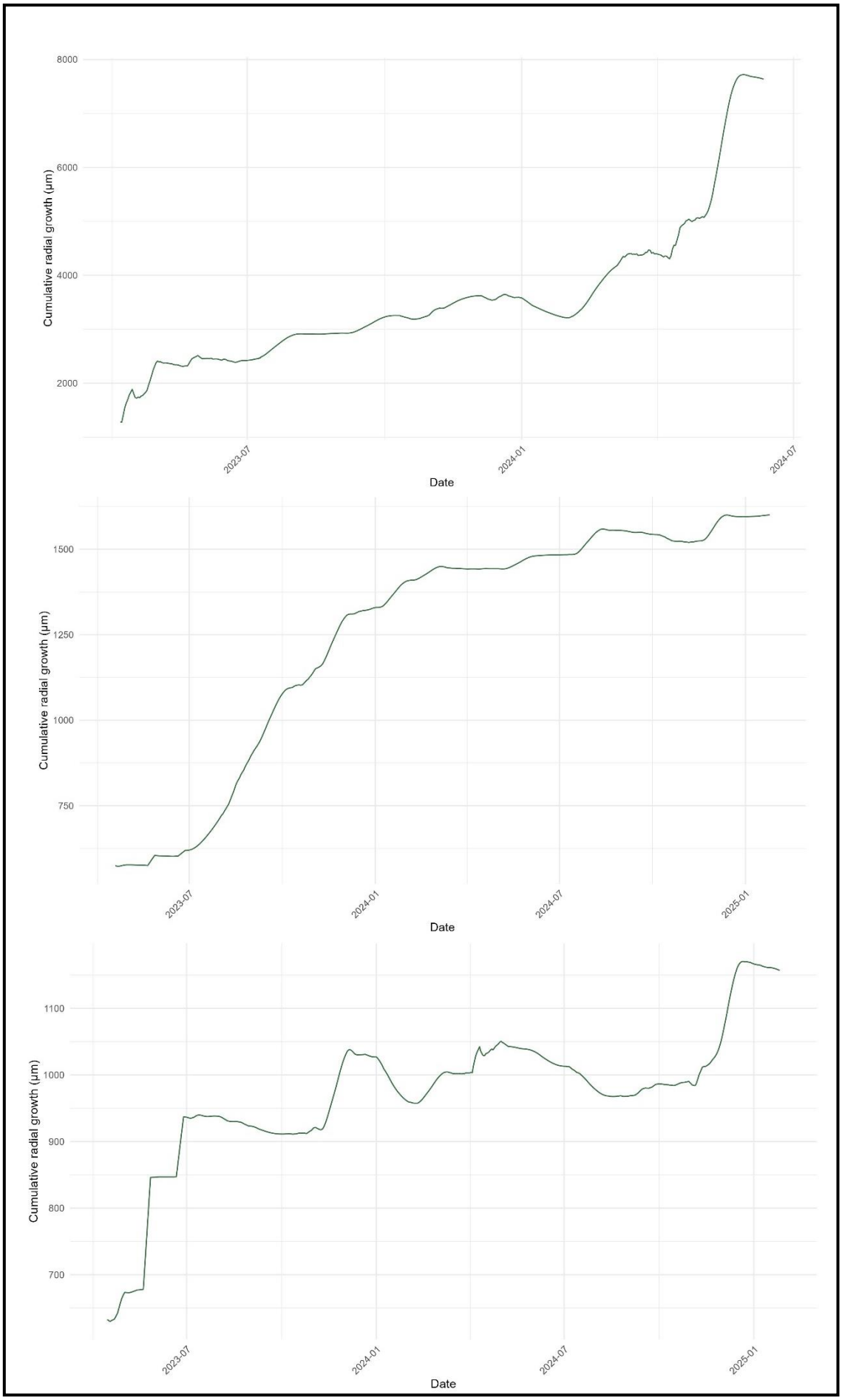

Figure A2: Examples of three dendrometer curves classified as 'others' and excluded from the analyses conducted in this study

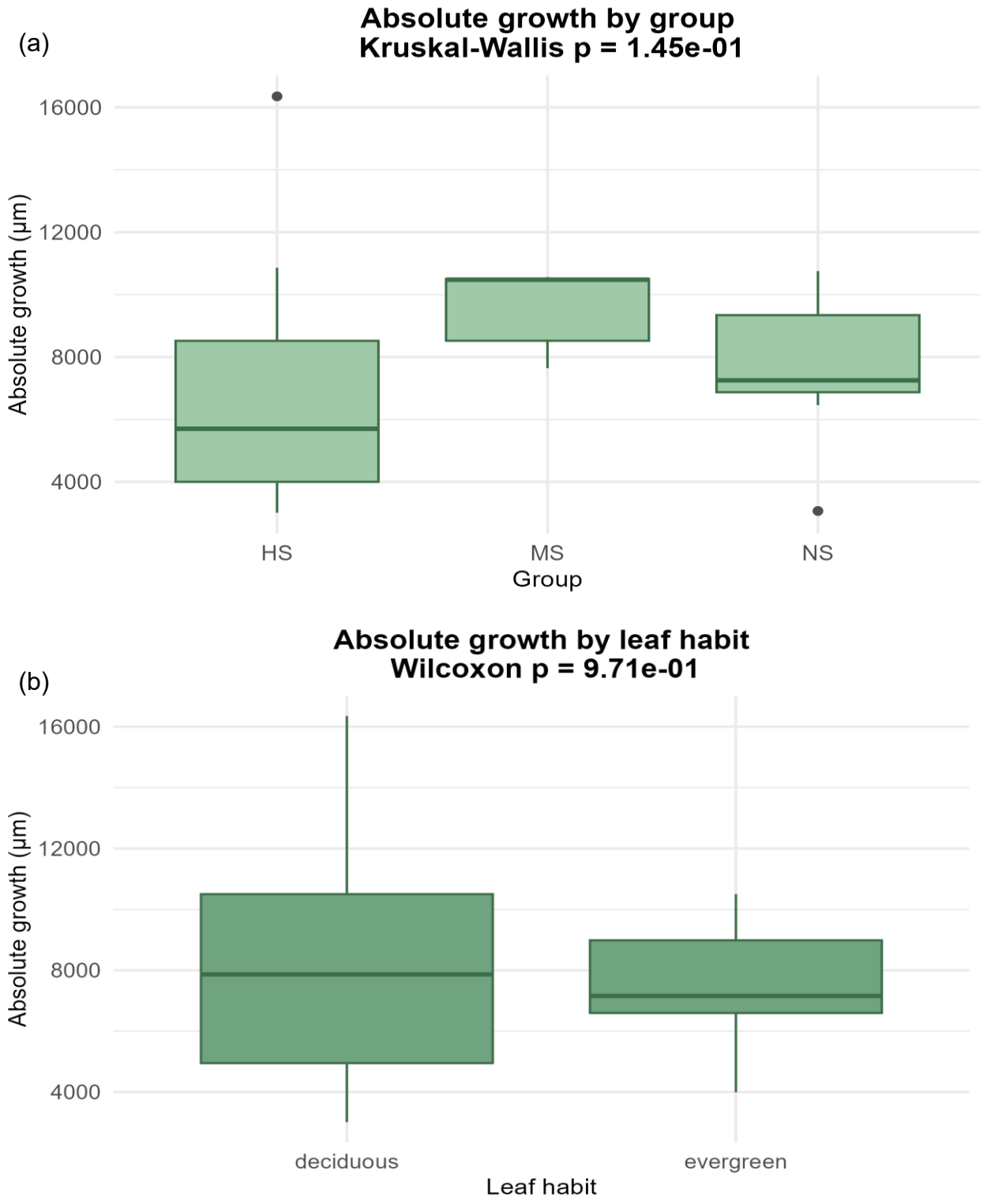

Figure A3: Boxplots showing the distribution of absolute growth (µm) across different leaf habits (evergreen and deciduous) (a) and growth patterns (Highly seasonal - HS, Moderately seasonal - MS, and Non-seasonal - NS) (b). Kruskal-Wallis (a) and Wilcoxon rank-sum (b) tests were performed to assess group differences, with associated p-values reported.

ID	Species	Familly	Leaf habits	Pattern	DBH (cm)	H (m)	Basal area (m^2)	Wood density (g/cm^3)	Absolute growth (um)
92232066	*Albizia ferruginea*	Fabaceae	deciduous	HS	27,9	23,6	0,06	0,54	12074
92232061	*Albizia gummifera*	Fabaceae	deciduous	HS	81,4	25,55	0,52	0,5	6150,18
92232047	*Albizia gummifera**	Fabaceae	deciduous	HS	117,5	33	1,08	0,5	9055,71
92232048	*Albizia gummifera**	Fabaceae	deciduous	HS	117,5	33	1,08	0,5	8824,85
92232021	*Dialium pachyphyllum*	Fabaceae	evergreen	HS	23,9	21	0,04	0,85	7340,87
92232023	*Dialium pachyphyllum*	Fabaceae	evergreen	HS	53,7	23,45	0,23	0,85	3990,14
92232081	*Irvingia gabonensis*	Irvingiaceae	deciduous	HS	NA	46,1	NA	0,74	2873,73
92232033	*Prioria balsamifera*	Fabaceae	deciduous	HS	77,2	36,8	0,47	0,4	6904,31
92232086	*Prioria balsamifera*	Fabaceae	deciduous	HS	73	32,5	0,42	0,4	3858,39
92232022	*Pterocarpus tinctorius*	Fabaceae	deciduous	HS	37,3	25,55	0,11	0,8	16350,12
92232043	*Terminalia superba*	Combretaceae	deciduous	HS	52,5	33,5	0,22	0,45	4033,88
92232062	*Terminalia superba*	Combretaceae	deciduous	HS	95	32,5	0,71	0,45	3010,14
92232003	*Zanha golungensis***	Sapindaceae	deciduous	HS	108,3	26,25	0,92	0,73	5252,61
92232009	*Zanha golungensis***	Sapindaceae	deciduous	HS	108,3	26,25	0,92	0,73	10860,71
92232064	*Ganophyllum giganteum*	Sapindaceae	evergreen	MS	87,2	31,45	0,60	0,71	10500,6
92232025	*Hannoa klaineana*	Simaroubaceae	NA	MS	66,2	26	0,34	0,25	7642,34
92232045	*Milicia excelsa*	Moraceae	deciduous	MS	68,4	28,65	0,37	0,55	10478,53
92232030	*Piptadeniastrum africanum*	Fabaceae	deciduous	MS	86,9	34,85	0,59	0,53	8521,19
92232010	*Piptadeniastrum africanum****	Fabaceae	deciduous	MS	102	38,75	0,82	0,53	10561,14
92232029	*Piptadeniastrum africanum****	Fabaceae	deciduous	MS	102	38,75	0,82	0,53	13089,56
92232082	*Blighia welwitschii*	Sapindaceae	deciduous	NS	79,1	47,75	0,49	0,72	9274,84
92232028	*Dacryodes X*	Burseraceae	NA	NS	58,5	36	0,27	NA	5673,73
92232074	*Funtumia elastica*	Apocynaceae	evergreen	NS	46,4	24,45	0,17	0,5	9543,35
92232057	*Ganophyllum giganteum*	Sapindaceae	evergreen	NS	88,1	30,9	0,61	0,71	7010,59
92232068	*Guarea cedrata*	Meliaceae	evergreen	NS	61,9	34,15	0,30	0,52	7300,31
92232050	*Maranthes glabra*	Chrysobalanaceae	deciduous	NS	98,6	21,2	0,76	0,84	3066,31
92232008	*Ongokea gore*	Olacaceae	evergreen	NS	78,3	30,55	0,48	0,72	6457,36
92232065	*Piptadeniastrum africanum*	Fabaceae	deciduous	NS	89,7	38,8	0,63	0,53	10754,28
92232016	*Staudtia kamerunensis*	Myristicaceae	deciduous	NS	91,2	37,35	0,65	0,71	7205,28

Table A1: Summary table of the trees selected after data cleaning, including the dendrometer ID, species, family, leaf habit (deciduous or evergreen), seasonal growth pattern (Highly seasonal - HS, Moderately seasonal - MS, or Non-seasonal - NS), diameter at breast height (DBH, cm), height (H, m), basal area (m^2), wood density (g/cm^3), and absolute growth over the full data period (in µm). The asterisks indicate that both dendrometers are installed on the same tre

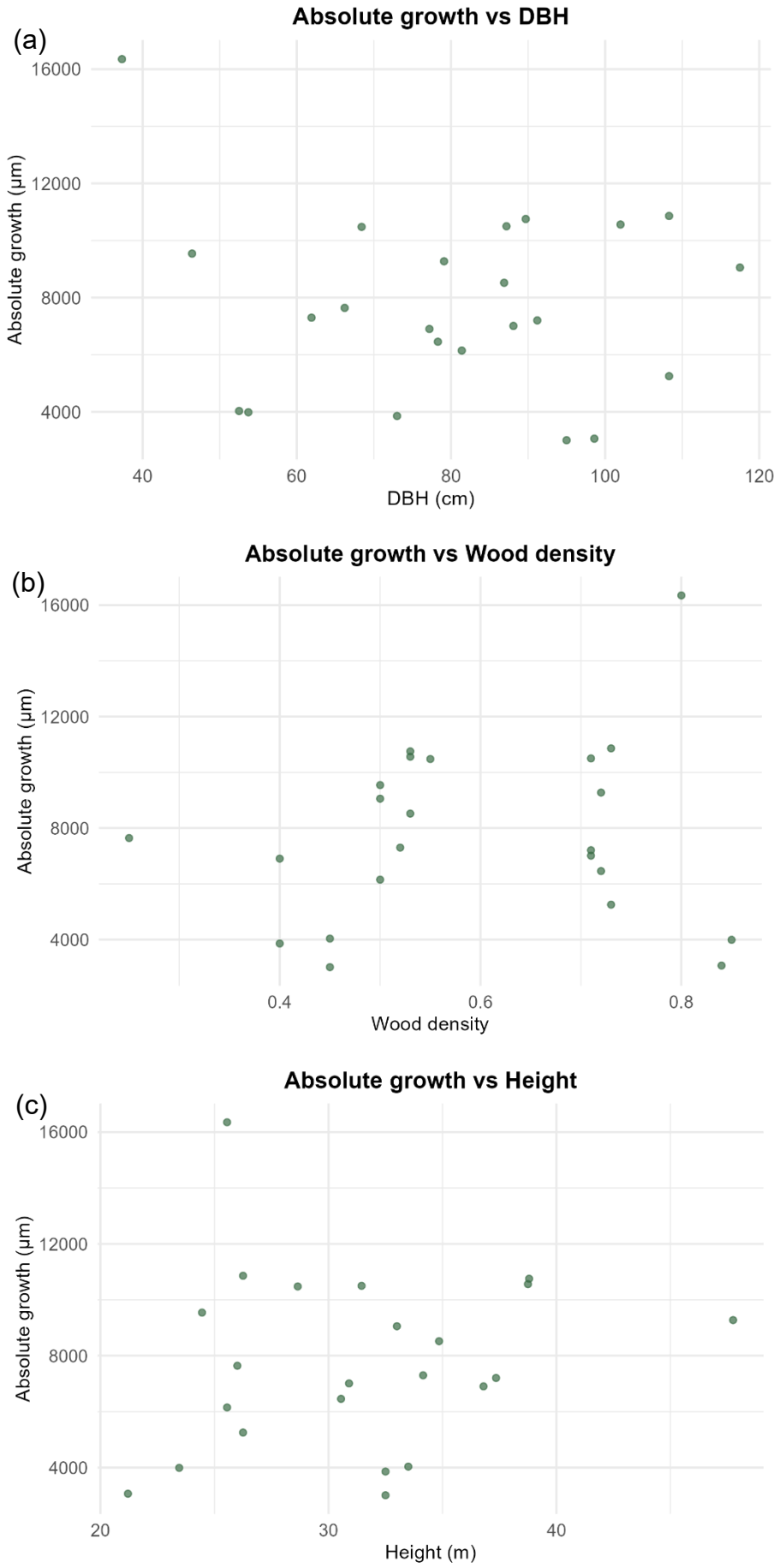

Figure A4: Scatterplots illustrating the relationships between absolute growth (µm) and diameter at breast height (DBH, a), wood density (g/cm³, b), and height (m, c). Each point represents one tree. These plots aim to visualise variability and explore potential trends between the variables

ID	nBP	Mean score	Max score	Min score
92232003	4	0,97	0,99	0,96
92232005	1	0,80	0,80	0,80
92232009	4	0,91	0,94	0,85
92232010	3	0,96	0,98	0,94
92232011	2	0,93	0,99	0,87
92232018	3	0,79	0,99	0,49
92232021	3	0,94	0,98	0,86
92232022	4	0,89	0,95	0,84
92232023	3	0,93	0,97	0,88
92232025	2	0,97	0,97	0,96
92232027	1	0,99	0,99	0,99
92232029	3	0,92	0,98	0,88
92232030	4	0,95	1,00	0,88
92232033	3	0,96	0,99	0,91
92232043	4	0,85	0,95	0,75
92232045	4	0,96	0,99	0,87
92232047	4	0,95	0,99	0,87
92232048	3	0,87	0,99	0,76
92232049	1	0,96	0,96	0,96
92232059	4	0,92	0,99	0,86
92232061	3	0,95	0,99	0,90
92232062	3	0,92	0,95	0,87
92232064	4	0,90	0,98	0,82
92232066	2	0,89	0,91	0,88
92232069	3	0,97	0,99	0,93
92232071	1	0,76	0,76	0,76
92232072	2	0,96	1,00	0,93
92232075	4	0,96	1,00	0,89
92232081	2	0,89	0,95	0,84
92232086	3	0,88	0,99	0,69
92232087	6	0,93	0,98	0,88
92232089	3	0,97	0,99	0,94
92232090	2	0,90	0,97	0,83

Table A2: Mean, minimum and maximum score of the breakpoint detected and selected

ID	Species	Familly	Leaf habits	Start DOY	End DOY	GR (um/day)	nGROW	Absolute growth (um)
92232003	*Zanha golungensis**	Sapindaceae	deciduous	340	143	18,78	168	3155,04
92232009	*Zanha golungensis**	Sapindaceae	deciduous	341	136	33,22	160	5315,2
92232021	*Dialium pachyphyllum*	Fabaceae	evergreen	295	119	22,29	189	4212,81
92232022	*Pterocarpus tinctorius*	Fabaceae	deciduous	329	102	66,57	138	9186,66
92232023	*Dialium pachyphyllum*	Fabaceae	evergreen	288	130	14,02	207	2902,14
92232033	*Prioria balsamifera*	Fabaceae	deciduous	250	128	18,98	243	4612,14
92232043	*Terminalia superba*	Combretaceae	deciduous	305	91	8,74	151	1319,74
92232047	*Albizia gummifera***	Fabaceae	deciduous	365	112	50,99	112	5710,88
92232048	*Albizia gummifera***	Fabaceae	deciduous	4	148	39,88	144	5742,72
92232061	*Albizia gummifera*	Fabaceae	deciduous	4	144	32,24	140	4513,6
92232062	*Terminalia superba*	Combretaceae	deciduous	47	190	16,15	143	2309,45
92232066	*Albizia ferruginea*	Fabaceae	deciduous	38	182	49,17	144	7080,48
92232081	*Irvingia gabonensis*	Irvingiaceae	deciduous	2	156	11,73	154	1806,42
92232086	*Prioria balsamifera*	Fabaceae	deciduous	12	130	16,35	118	1929,3

Table A3: Key metrics from the breakpoint analysis for each tree exhibiting a highly seasonal pattern: the day of year marking the start (start DOY) and end (end DOY) of the growth period, the number of growth days (nGROW), the growth rate (GR, in µm/day), and the absolute growth (in µm) during the growth period from August 2023 to August 2024.

ID	Species	Familly	Leaf habits	Start DOY	End DOY	nGROW	GR (um/day)	Absolute growth (um)
92232064	*Ganophyllum giganteum*	Sapindaceae	evergreen	7	117	110	36,87	4055,7
92232025	*Hannoa klaineana*	Simaroubaceae	NA	38	229	191	22,55	4307,05
92232045	*Milicia excelsa*	Moraceae	deciduous	303	148	210	25,41	5336,1
92232030	*Piptadeniastrum africanum*	Fabaceae	deciduous	302	133	196	29,96	5872,16
92232010	*Piptadeniastrum africanum***	Fabaceae	deciduous	291	112	186	31,89	5931,54
92232029	*Piptadeniastrum africanum***	Fabaceae	deciduous	298	119	186	28,71	5340,06

Table A4: Key metrics from the breakpoint analysis for each tree exhibiting a moderately seasonal pattern: the day of year marking the start (start DOY) and end (end DOY) of the growth period, the number of growth days (nGROW), the growth rate (GR, in µm/day), and the absolute growth (in µm) during the growth period from August 2023 to August 2024.

ID	*Species*	Familly	Leaf habits	GR (um/day)	Absolute growth (um)
92232008	*Ongokea gore*	Olacaceae	evergreen	10,09	6457,36
92232016	*Staudtia kamerunensis*	Myristicaceae	deciduous	11,28	7205,28
92232028	*Dacryodes X*	Burseraceae	NA	8,88	5673,73
92232050	*Marantus glabra*	Chrysobalanaceae	deciduous	4,74	3066,31
92232057	*Ganophyllum giganteum*	Sapindaceae	evergreen	11,18	7010,59
92232065	*Piptadeniastrum africanum*	Fabaceae	deciduous	16,98	10754,28
92232068	*Guarea cedrata*	Meliaceae	evergreen	10,81	7300,31
92232074	*Funtumia elastica*	Apocynaceae	evergreen	15,02	9543,35
92232082	*Blighia welwitschii*	Sapindaceae	deciduous	14,88	9274,84

Table A5: Key metrics for each tree exhibiting a non-seasonal pattern: the growth rate (GR, in µm/day) and the absolute growth (in µm), calculated over the entire study period.

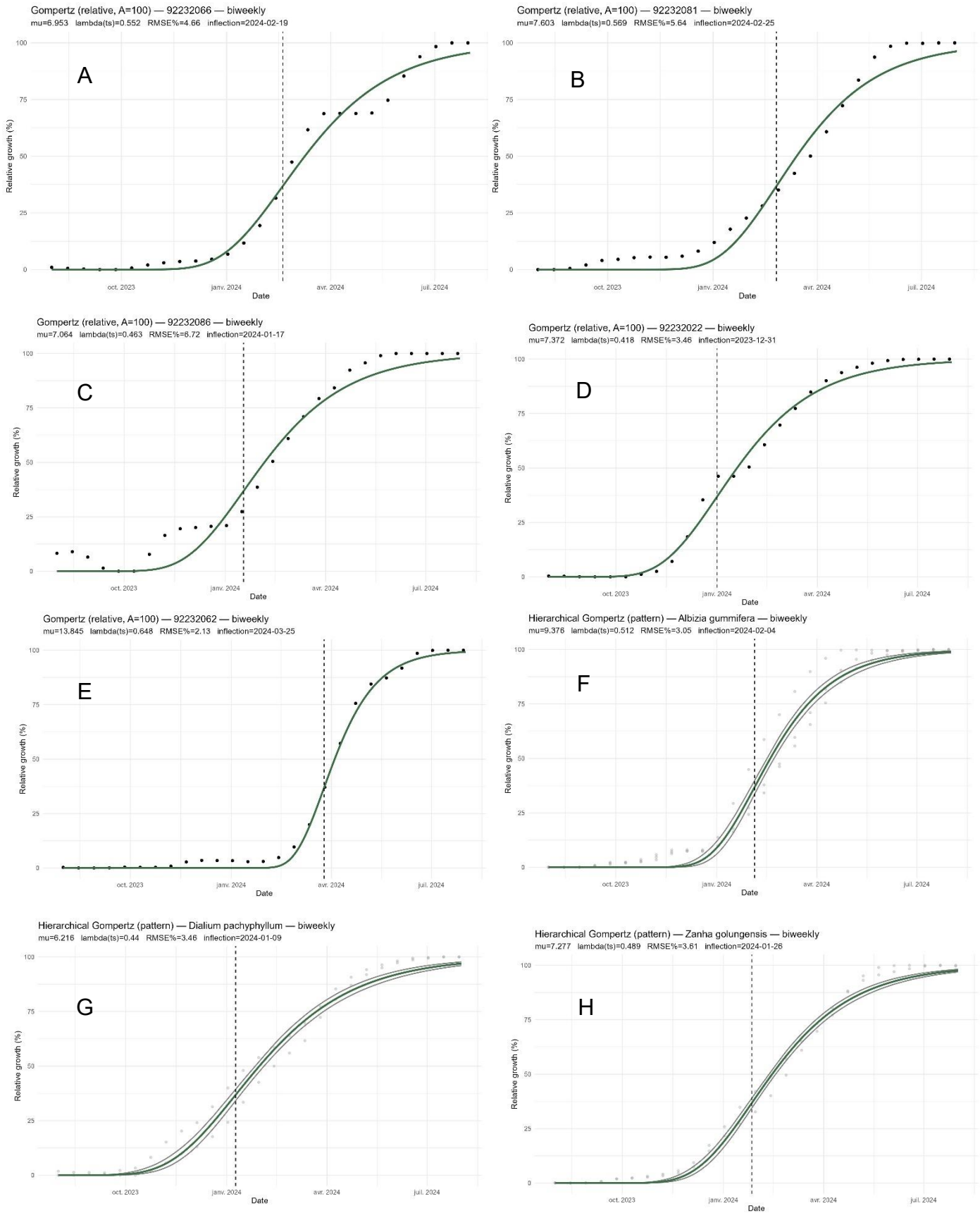

Figure A5: Gompertz model for all the species classified highly seasonal: (A) Albizia ferruginea, (B) Irvingia gobensis, (C) Prioria Balsamifera, (D) Pterocarpus tinctorius, (E) Terminalia superba, (F) Albizia gummifera, (G) Dialium pachyphyllum and (H) Zanha golugensis.